Biochemical Pharmacology 222 (2024) 116097

Contents lists available at ScienceDirect

Biochemical Pharmacology

journal homepage: www.elsevier.com/locate/biochempharm

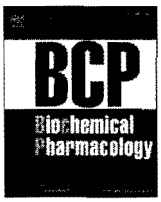

Proliferation and migration of PC-3 prostate cancer cells is counteracted by PPARγ-cladosporol binding-mediated apoptosis and a decreased lipid biosynthesis and accumulation

Roberta Rapuano [a], Alessio Riccio [a], Antonella Mercuri [a], Jessica Raffaella Madera [a], Sabrina Dallavalle [b], Salvatore Moricca [c], Angelo Lupo [a,*]

[a] Dipartimento di Scienze e Tecnologie, Università del Sannio, Via dei Mulini, 42, 82100 Benevento, Italy
[b] Dipartimento di Scienze per gli Alimenti, la Nutrizione e l'Ambiente, Università degli Studi di Milano, via Celoria 2, 20133 Milano, Italy
[c] Dipartimento di Scienze e Tecnologie Agrarie, Alimentari, Ambientali e Forestali (DAGRI), Università degli Studi di Firenze, Piazzale delle Cascine 28, 50144 Firenze, Italy

ARTICLE INFO

Keywords:
Cladosporols
PPARγ agonists
Proliferation
Migration
Apoptosis
Lipogenesis

ABSTRACT

Objectives: Chemoprevention, consisting of the administration of natural and/or synthetic compounds, appears to be an alternative way to common therapeutical approaches to preventing the occurrence of various cancers. Cladosporols, secondary metabolites from *Cladosporium tenuissimum*, showed a powerful ability in controlling human colon cancer cell proliferation through a peroxisome proliferator-activated receptor gamma (PPARγ)-mediated modulation of gene expression. Hence, we carried out experiments to verify the anticancer properties of cladosporols in human prostate cancer cells. Prostate cancer represents one of the most widespread tumors in which several risk factors play a role in determining its high mortality rate in men.

Materials and methods: We assessed, by viability assays, PPARγ silencing and overexpression experiments and western blotting analysis, the anticancer properties of cladosporols in cancer prostate cell lines.

Results: Cladosporols A and B selectively inhibited the proliferation of human prostate PNT-1A, LNCaP and PC-3 cells and their most impactful antiproliferative ability towards PC-3 prostate cancer cells, was mediated by PPARγ modulation. Moreover, the anticancer ability of cladosporols implied a sustained apoptosis. Finally, cladosporols negatively regulated the expression of enzymes involved in the biosynthesis of fatty acids and cholesterol, thus enforcing the relationship between prostate cancer development and lipid metabolism dysregulation.

Conclusion: This is the first work, to our knowledge, in which the role of cladosporols A and B was disclosed in prostate cancer cells. Importantly, the present study highlighted the potential of cladosporols as new therapeutical tools, which, interfering with cell proliferation and lipid pathway dysregulation, may control prostate cancer initiation and progression.

1. Introduction

Prostate cancer is the most widespread cancer in men in the United States beyond skin cancer. The American Cancer Society foresees that in the United States, by 2023, 288,300 new cases of prostate cancer will occur and about 34,700 deaths will occur among prostate cancer patients [1]. During his lifetime, one in seven men will be diagnosed with prostate cancer. The risk of prostate cancer is higher in older men, and, indeed, about the 65% of new cases are diagnosed in men aged between 55 and 74 years. It is very rare to diagnose a case of prostate cancer before the age of 40. The average age at diagnosis is about 66 years [1]. In Europe, accumulated data from studies, performed until

Abbreviations: AR, Androgen receptor; CCK-8, Cell Counting Kit-8; CRC, colorectal cancer; DMEM, Dulbecco's Modified Eagle Medium; DMSO, Dimethylsulfoxide; FACS, fluorescence-activated cell sorting; FBS, foetal bovine serum; FCS, foetal calf serum; IBMX, 3-isobutyl-1-methylxanthine; MDI, differentiation medium; mRNA, messenger RNA; NRs, Nuclear receptors; PPAR, peroxisome proliferator-activated receptor; PPARγ, peroxisome proliferator-activated receptor gamma; PPRE, PPAR response element; RPMI, Rosewell Park Memorial Institute 1640 Medium; RGZ, rosiglitazone.

* Corresponding author.
E-mail address: lupo@unisannio.it (A. Lupo).

https://doi.org/10.1016/j.bcp.2024.116097
Received 22 November 2023; Received in revised form 15 February 2024; Accepted 26 February 2024
Available online 28 February 2024

2021, indicated that about 22% of newly diagnosed cancers in men, across all ages, consisted of prostate cancer. Lung and colorectal cancers, which constituted just over 50% of cancers in men, soon follow. Prostate cancer was responsible for 10% of cancer deaths in males, translating into an age-standardized incidence rate of 148.1 and an associated mortality rate of 38.2 per 100.000 cases [2].

Although some risk factors for prostate cancer have so far been highlighted (age, diet, smoking, genetic mutations, inflammation and sexually transmitted infections), we need to learn much more about them and more extended studies will be necessary to describe how these factors induce prostate cells to become cancer cells [3]. Prostate cancer progression has also been postulated to be promoted by a high-calorie diet [4,5]. However, bits of evidence, that definitively sustain the association between a high-calorie diet and prostate cancer, still need to be consolidated [6]. Recently, two studies from independent laboratories established a close relationship between dietary lipids and prostate cancer progression to metastasis in mouse tumor models [7,8]. However, understanding the factors that contribute to prostate cancer for an early diagnosis is usually a crucial step in also determining the stage of prostate cancer and deciding on the best patient's treatment options. Surgery, radiation therapy, hormone therapy, chemotherapy and immunotherapy are the most efficient approaches used to treat prostate cancer. Several studies have pointed out the benefits of natural molecules in managing and treating prostate cancer. Compounds present in extracts from soy, pomegranate, broccoli and green tea are also able to limit prostate cancer progression after surgery [9]. America's biopharma research companies are just now testing about one thousand new drugs, derived from plants, fungi and microorganisms, to fight different types of cancer that affect millions of people across the world [10,11]. The increased comprehension of molecular mechanisms underlying cancer, metabolism and other biological aspects has aroused the interest in identifying new molecules able to selectively target proteins involved in molecular pathways impaired by cancer and metabolic diseases, thus avoiding adverse effects associated with conventional medicine.

The specificity of the action of natural compounds depends strictly on their ability to bind a receptor to activate or repress different signaling pathways. Nuclear receptors (NRs) constitute an evolutionarily well-conserved class of proteins able to sense the external signals and to act as transcription factors regulating the expression of target genes. The nature and structure of ligands confer to NRs the ability to respond to injuries from the environment and to selectively stimulate pathways to modulate metabolism, cell growth, differentiation and other functions. It is well known that ligands of NRs are common drugs used to alleviate several diseases and constitute 10–20% of the pharmaceutical market worldwide [12,13]. Ligands that bind to NRs originate from inside the cell and also from the outside environment. Between these latter we can distinguish natural ligands obtained from microrganisms (bacteria, algae, fungi) and plants, or synthetic ligands produced in laboratories.

Findings from recent reports focused on the role of cladosporols, secondary metabolites derived from *Cladosporium tenuissimum*, in controlling colorectal cancer (CRC) cell proliferation and also modulating adipocyte differentiation in 3T3-L1 murine preadipocytes. Particularly, we found that proliferation, migration and invasion of HT-29 colorectal cancer cells were inhibited by conditioned medium from cladosporol-treated 3T3-L1 mature adipocytes compared to the preadipocyte conditioned medium [14–17]. These results, indeed, suggesting the relationship between metabolism of lipids and their accumulation and colon cancer promotion, are consistent also with the numerous evidences indicating the role of obesity and periprostatic adipose tissue in prostate cancer aggressiveness and mortality [18–20].

We further demonstrated that cladosporols displayed these functions, acting as peroxisome proliferators-activated receptors gamma (PPARγ) ligands in a different cellular milieu. Belonging to the first class of the NR superfamily, PPARs regulate a wide range of biological processes including glucose and lipid metabolism, differentiation, cell growth and inflammation in different tissues [21,22]. On the basis of these reasoning, we proposed here that cladosporols A and B, as PPARγ ligands, interfering with two relevant pathological processes (cell proliferation and lipid pathways dysregulation), could be efficient therapeutic tools in controlling of both cancer and metabolism to prevent and manage diabetes, obesity and cancer [23,24]. In this work, indeed, by viability assays, we investigated whether cladosporols A and B inhibited proliferation of prostate cancer cells, especially metastatic PC-3 cells. In addition, we found that the antiproliferative effects of cladosporols A and B are mediated by PPARγ binding. By Annexin V assays and western blotting experiments, we also demonstrated that cladosporol-bound PPARγ stimulates prostate cancer cell apoptosis through regulation of caspase-3, Bcl-2 and caspase-9 protein expression. Cladosporols A and B have been found to inversely regulate the synthesis and secretion of leptin and adiponectin in 3T3-L1 cells, thus influencing the proliferation and migration of PC-3 prostate cancer cells cultured in the medium from cladosporol-treated 3T3-L1 mature adipocytes. Finally, cladosporols A and B treatments also affected some enzyme activities involved in the biosynthesis of fatty acids and cholesterol, suggesting that the impairment of lipid metabolism may result in the arrest of prostate cancer cell proliferation.

2. Materials and Methods

2.1. Cell lines

3T3-L1 preadipocytes were a gift from Prof. Francesco Beguinot and Prof. Claudia Miele of the Department of Translational Medical Sciences, "Federico II" University of Naples, Italy. PNT-1A and LNCaP prostate cells were provided by Prof. Gabriella Castoria (Università della Campania "L. Vanvitelli" Dip. Medicina di Precisione via L. De Crecchio, 7 80,138 Napoli, Italy). PC-3 cells were provided by ATCC (Manassas, Virginia). PNT-1A, LNCaP and PC-3 prostate cells were selected as experimental models because they show a specific genetic profile and distinctive biological features. PNT-1A cells have been derived from normal prostates with mild hyperplasia. These cells are responsive to androgen hormones, synthetize and secrete PSA and are non-tumorigenic in nude mice [25]. For these reasons, we considered this cell type as normal prostate cells and used them as control of the proliferation assays. PC-3, and LNCaP cells are the best-known prostatic carcinoma cell lines [26]. LNCaP cells have a high affinity for nuclear androgen receptor (AR) and respond to androgens, that stimulate their growth, and form tumors in nude mice. Male mice develop tumors earlier than female mice, confirming their androgen responsiveness [25,26]. PC-3 cells, on the contrary, do not express PSA and are generally assumed to be hormone unresponsive. In summary, LNCaP cells are more differentiated than PC-3 cells, which, in turn, show a more aggressive phenotype. 3T3-L1 cells were grown as monolayers in Dulbecco's Modified Eagle's Medium (DMEM) and PC-3, PNT-1A and LNCaP Rosewell Park Memorial Institute 1640 Medium (RPMI) supplemented with 1% (v/v) penicillin/ streptomycin, 10% (v/v) Fetal bovine serum (FBS) and 1% (v/v) L-glutamine. They were seeded in a 75 cm^2 culture flask at a density of 6.0 x 10^4 cells in the medium supplemented with 1% (v/v) penicillin/streptomycin and 10% FBS. For their maintenance, these cells were cultured in 100 mm plates at 70–80% confluence in a 5% CO_2-humidified atmosphere at 37 °C.

2.2. Fungus production and purification of cladosporols A and B

The selected fungal strain ITT21 from the destructive mycoparasite *Cladosporium tenuissimum* Cooke, recovered from *Cronartium flaccidum* aeciospore samples collected in 1996 on *Pinus pinaster* in Tuscany (Italy), was employed [27]. The fungus effectively restricts the development of diseases in the field by parasitizing spores of rusts and other harmful plant fungal pathogens [28]. The fungus was grown in batch of 40 Roux

flasks containing 100 ml MPGGA (malt extract, peptone, glucose, glycerol, agar, 20:2:20:10:15 g l-1). After two weeks the cultures were extracted twice with EthylAcetate-Methanol (EtOAc–MeOH) (99:1). The extracts (1.4 g) were dried over Sodium Sulfate (Na2SO4), evaporated to dryness and purified by column chromatography (eluent: Methilene Chloride (CH2Cl2) /Methanol (MeOH) from 99:1 to 85:15). Collected fractions were further purified by Performance Liquid Chromatography (PLC) to give 310 mg of cladosporol A as a white powder, mp 192–195 °C dec.; [a]D + 136 (MeOH, c 0.1); Rf 0.4 (CH2Cl2:MeOH 15:1) and 10 mg of cladosporol B as a brown powder, mp 175–180 °C; [a]D + 58 (Chloroform (CHCl3), c 0.05); Rf 0.7 (CH2Cl2:MeOH 15:1). The spectroscopic data matched with those reported in the literature [16]. In accordance with the protocols already adopted, cladosporol A, cladosporol B, rosiglitazone (RGZ) and GW9662 were dissolved in DMSO, mixed with fresh medium to achieve the final concentration and injected into cells at 70% confluence [14–17]. DMSO was used as a control in medium with concentrations less than 0.1%. The cells were treated with increasing concentrations of compounds for different times, as indicated.

2.3. Antibodies and reagents

The manufacturer, the catalog number and the dilution used of the antibodies mentioned in the work are reported below. Antibodies against total PPARγ (SC-7273 1:500), Bcl-2 (SC7382 1:1000), MMP9 (SC-393859 1:1000), SREBP1 (SC-13551 1:1000), FABP4 (SC-271519 1:1000), anti-goat (IgG HRP-conjugated Santa Cruz SC-2354 1:2000) were purchased from Santa Cruz Biotechnology (Santa Cruz, CA, USA). Antibodies against PPARγ2 (PA1-824 1:1000), AdipoR1(PA1-059 1:1000) were purchased from Thermo Fisher Scientific (Waltham, Massachusets, USA). Antibodies against Androgen Receptor (#4967 1:5000), cyclin D1 (#2978S 1:1000), FAS (#4233 1:1000), ACC (#36625 1:1000), E-cadherin (#24E10 1:1000), caspase-3 (#9662 1:1000), cleaved caspase 3 (96615 1:1000), caspase-9 (#9508 1:1000), adiponectin (#2789 1:1000), β-actin (#4967 1:5000), anti-rabbit (IgG HRP-conjugated Cell Signaling #7074 1:2000) and anti-mouse (IgG HRP-conjugated Cell Signaling #7076 1:2000) secondary antibodies were purchased from Cell Signaling Technology (Cell Signaling Technology, Danvers, Massachusetts, USA). Antibodies against β-catenin (BD 610,153 1:1000) was purchased from Becton Dickinson (Franklin Lake, New Jersey, USA). Antibodies against leptin (Ab-16227 1:1000), HMG-CoAr (AbCam Ab-214018 1:1000) were purchased from Labcam (Cambridge,UK). Description of all the consumables and reagents was reported below. ECL Western blotting detection kits (BIORAD #1705061), Tween 20 (BIORAD #1610156), Acrilamide 30% (BIORAD #1610156), TEMED (N,N,N,N,tetramethylethylenediammine) (BIORAD #1610801), Sodium Dodecyl Sulfate, SDS (BIORAD #1610416), Turbo transfer kit (BIORAD #1704270), PVDF membrane (BIORAD #1620177), Precision dual marker (BIORAD #1610374) and Loading Laemli buffer 4x (BIORAD #1610747) were purchased from Biorad (Hercules, California, USA). Dimethylsulfoxide, DMSO (SERVA #20385.02), Bovin serum albumin, BSA (SERVA 11920.04) were purchased from Serva (Heidelberg, Deutschland). Phosphate-buffered saline, PBS (MERCK #D8537), FBS (MERCK #50615), GW9662 (MERCK #M6191), Rosiglitazone (MERCK #R2408), dexamethasone (MERCK #265005), insuline (MERCK #15500), Isobutylmethylxanthine, IBMX (MERCK 15879), Ammonium persulphate, APS (MERCK #A3678), Ponceau solution (MERCK #P7170), Oil Red O reagent (MERCK #O0625) were purchased from Merck (Darmstadt,). Penicillin-streptomycin (LONZA #DE17-602E), L-glutamine (LONZA#BE17-605E) were purchased from Lonza (Basel, Schweiz). DMEM (GIBCO #11965092), RPMI (GIBCO #21875034), trypsin-EDTA (GIBCO #25300054) were obtained from Gibco (Carlsbad, CA, USA). Lipofectamine 3000 reagent (INVITROGEN #L3000001) was from Invitrogen (Carlsbad, CA, USA). Annexin V-Fitc Apoptosis Detection Kit (BD Pharmingen™) was from Becton and Dickinson (Franklin Lakes, New Jersey, USA). OranguTM Cell Counting Solution guidance systems (CCK-8 OR01-1000) was obtained from Cell Guidance Systems (Cambridge, UK).

2.4. Cell viability

To measure cell proliferation after exposure to cladosporols A and B, prostate cells were cultured in a 12-well plate at a density of 10^4 cells/cm^2. PNT-1A, LNCaP and PC-3 cells were treated or not with 1, 5 and 10 μM of rosiglitazone, cladosporol A and cladosporol B for 24, 48 and 72 hrs. After cladosporol treatment, the cells were washed with PBS, trypsinized, collected in culture medium and counted in Bürker chamber. The viability of the prostate cells was further evaluated using the CCK-8 Assay Orangu™ (Cell Guidance Systems, Babraham, England). Briefly, prostate cells were plated in 96-well plates at density of 10^4 cells/cm^2. At 70% confluence, 10% (v/v) of Orangu™ solution was added to each sample. After 3 hrs of incubation, in a 5% CO2 humidified atmosphere, at 37 °C, the absorbance was read at 450 nm in a standard plate reader (TECAN Infinite 200 PRO, Austria).

2.5. Overexpressing and silencing of PPARγ in PNT1-A and PC-3 prostate cells

After 2 days of expansion, PNT1-A prostate cells were transiently transfected with the PCDNA3 recombinant plasmid, bearing the entire cDNA fragment encoding for PPARγ under the control of Cytomegalovirus (CMV) promoter, by Lipofectamine 3000 reagent, in accordance with the manufacturer's instructions. After 24 hrs the cells were treated with both cladosporols (10 μM). After further 48 hrs, cells were collected and used to evaluate, by western blotting, the expression of total PPARγ and also to measure cell viability of prostate cells using the CCK-8 Assay. For transient PPARγ knock-down, a mixture of siRNA, targeting PPARγ on exon 5 of the gene (Human PPARγ DsiRNA duplex (HSCRNAIN005037.12.3) from Integrated DNA Technologies (IDT) (Coralville, Iowa, USA)), was used in transient transfection experiments of PC-3 cells by using Lipofectamine 3000 reagent. After 48 hrs cells were collected and used to evaluate, by western blotting, the expression of total PPARγ and to measure cell viability of prostate cells by using the CCK-8 Assay.

2.6. Annexin V/PI staining for apoptosis analysis

To analyze the apoptotic effects of both cladosporols on PC-3 metastatic prostate cancer cells, Annexin V-FITC/propidium iodide staining was used. According to the manufacturer's protocol, PC-3 cells were treated with drugs or vehicle control (0.5% DMSO) for 48 hrs and then washed with cold PBS three times and resuspended in 200 μL binding buffer. Successively, 10 μL of Annexin V-FITC and 10 μL of propidium iodide were added and the reactions were carried out for 30 min, at 4 °C and in the dark. Samples were analyzed by fluorescence-activated cell sorting (FACS) using BD FACSCelesta™ Cell Analyzer.

2.7. Western blotting analysis

Treated and untreated cells were lysed in Ripa buffer (150 mM NaCl, 50 mM Tris-HCl, pH 7.6, 10 mM EDTA and 1% NP-40) also containing a protease inhibitor cocktail and then centrifuged at 17,000 Relative Centrifugal Force (RCF) for 10 min at 4 °C. The supernatant containing total proteins was quantified and in the most of assays 80 μg of each sample were separated on 12% SDS-PAGE. Western blotting assays were carried out as previously reported [13]. The proteins were then electrotransferred onto polivinilidenfluorure (PVDF) membranes. The

efficiency of the protein transfer was always appraised by protein visualization with Ponceau S. After incubation with primary antibodies and horseradish peroxide (HRP)-conjugated goat anti-rabbit and anti-mouse secondary antibodies, the relative intensity of the protein bands was measured using the Molecular Imager Chemi-Doc imaging system and evaluated using the Image Lab software (Bio-Rad, Hercules CA, USA).

2.8. 3 T3-L1 differentiation and PC-3 reconditioning

3T3-L1 preadipocytes were seeded in a 60 mm plate in a number of 8 x 10^4 cells at 60% confluence in an expansion medium (4.5 g/l glucose DMEM supplemented with 10% FBS and 1% penicillin/streptomycin). After two days, cells reached 100% confluence and were induced into differentiating with MDI (a mix of differentiation composed of DMEM plus 0.5 mM 1-methyl-3- isobutylxanthine (IBMX), 1 μM dexamethasone and 1 μg/ml insulin), MDI plus Rosiglitazone (MDI + RGZ), MDI plus Cladosporol A (MDI + CLA) and MDI plus Cladosporol B (MDI + CLB). After two days, the differentiation medium was removed and replaced each 2 days for 6 days with a maintenance medium containing DMEM, FBS and 1 μg/ml insulin, RGZ, CLA and CLB. In the experiment described in Fig. 7A and shown in Fig. 7 B and C only, for the last two days, CLA and CLB were removed from the medium (samples indicated as MDI-CLA and MDI-CLB). At day 8, all the media (from 3T3-L1 untreated, MDI, MDI + RGZ, MDI + CLA, MDI-CLA, MDI + CLB and MDI-CLB) were collected and used to culture PC-3 cells for 48 and 72 hrs.

2.9. Oil-Red O staining

Oil-Red O staining was performed to treat the prostate cell lines with 10% formaldehyde for 5 min at room temperature. The cells were washed with PBS 1X, incubated with isopropanol 60% for an additional 5 min and dried completely. Fixed cells were stained with Oil-Red O in 60% isopropyl alcohol solution for 1 h at room temperature. The stained lipid droplets in the cells were imaged with a light microscope at 20X magnification. Intracellular stored lipids were quantified by extracting Oil-Red O stain with 100% isopropyl alcohol and the absorbance was measured at 500 nm using a spectrophotometer to obtain a graph.

2.10. Wound-healing assay

PC-3 prostate cells were allowed to growth at a density of 5 × 10^5 cells/well until they were 100% confluent in an adherent monolayer. Successively, by a sterile yellow 10 μL Eppendorf tip a scratch in the central part of the well was done and three PBS washing of the cells in the plate was executed. The cells were then cultured in the absence or in presence of cladosporols (10 and 20 μM) and with reconditioned medium from 3T3-L1 for 48 and 72 hrs to verify a decrease in the wound area. The images of migrating cells were taken using a digital camera connected to the microscope (Nikon Eclipse Ts2 Inverted) at 10X magnification to evaluate the closure of wound area at 0, 48 and 72 hrs after treatment. The results were measured using the ImageJ software. The migration of PC-3 prostate cells was calculated as the percentage of the wound area at 48 and 72 hrs compared to the initial wound area at 0 hrs.

2.11. Statistical procedures

The experiments were carried out in triplicate with at least three/four independent replicates. Data from viability, flow cytometry, western blotting and transient transfection experiments were expressed as means ± SD. Data between three groups were assessed using the Wilcoxon-Mann-Whitney test. p-values less than 0.05 were considered significant.

3. Results

3.1. Cladosporols A and B differentially inhibited the growth of PNT-1A, LNCaP and PC-3 human prostate cell lines

To firstly investigate the anticancer role of cladosporols A and B, we evaluated the growth of different prostate cells (PNT-1A, LNCaP and PC-3) exposed to increasing concentrations of the compounds at different time points. PNT-1A, LNCaP and PC-3 prostate cells have been treated with increasing concentrations of cladosporol A (1, 5, 10 μM) for 24, 48 and 72 hrs. After this time, the surviving cells have been counted (Fig. 1). The number of cells was decreased in a dose- and time-dependent manner in all cell types and the reduction was particularly dramatic at the highest concentrations of cladosporol A. Moreover, the inhibitory effect of the drug was stronger in PC-3 cells than in PNT-1A and LNCaP cells. For example, the administration of 10 μM cladosporol A for 48 hrs inhibited PC-3 cell proliferation of about 70% and caused a 40% inhibition of LNCaP cell growth. At the same dosage and for the same time, cladosporol A provoked only 30% of inhibition of PNT-1A cell proliferation. Exposure to 10 μM cladosporol B for 48 hrs inhibited PC-3 cell proliferation of about 67% and caused 34% inhibition of LNCaP and 26% inhibition of PNT-1A cell growth. These results demonstrated that cladosporols A and B differentially inhibited PNT-1A, LNCaP and PC-3 prostate cell proliferation and preferred to arrest the growth of the most susceptible PC-3 cells. Treatment with 10 μM rosiglitazone (RGZ) for 48 hrs did not show the same effect on PNT-1A, LNCaP and PC-3 cell proliferation.

To confirm these results, we performed the CCK-8 assay, through which we determined the cytotoxicity effect of cladosporols A and B on prostate cancer cells. As expected, cladosporol A greatly reduced PC-3 cell proliferation with IC_{50} values of 4.75 μM, 3.87 μM and 2.52 μM for 24, 48 and 72 hrs long treatments, respectively, compared to the data obtained in PNT-1A (IC_{50} values of 6.54, 5.10 and 3.67 μM relative to 24, 48 and 72 hrs, respectively) and LNCaP (IC_{50} values of 7.91, 6.22 and 3.93 μM relative to 24, 48 and 72 hrs, respectively) treated cells (Fig. 2A **and** Table 1). Also the results obtained from the treatment of PNT-1A, LNCaP and PC-3 prostate cells with cladosporol B demonstrated that PC-3 cells are more sensitive than PNT-1A and LNCaP cells to the exposure to this more oxidized drug, as shown from the comparison of the IC_{50} values (compare IC_{50} values of 4.01, 3.03 and 2.07 μM found for PC-3 cells after 24, 48 and 72 hrs of treatment with those found for PNT-1A cells, namely 7.14, 4.25 and 3.39 μM, and for LNCaP cells 3.98, 3.26 and 2.6 μM) reported in Fig. 2B **and** Table 2. Altogether, these results demonstrated that cladosporols A and B inhibited PNT-1A, LNCaP and PC-3 prostate cell proliferation with the highest inhibitory effects for the most aggressive and metastatic PC-3 cells.

3.2. Inhibition of growth of human prostate cancer cells due to cladosporols A and B was mediated by PPARγ

To investigate the molecular mechanisms by which cladosporols A and B caused the above-described inhibition of prostate cell proliferation, we firstly decided to verify the basal level of PPARγ expression in PNT-1A, LNCaP and PC-3 prostate cells. As shown in Fig. 3A, a progressive increase of PPARγ expression was clearly evident, confirming the data from other laboratories which demonstrated a more intense PPARγ expression in metastatic PC-3 prostate cells when compared to PNT-1A and LNCaP [29,30]. We also analyzed, by western blotting assay, androgen receptor (AR) expression in the same cellular types because in several papers an inverse mode of expression of this receptor (compared to PPARγ) was demonstrated [31,32]. The results of Fig. 3B seemed to confirm that AR expression was higher in androgen-responsive PNT-1A and LNCaP cells when compared to the level of PC-3 cells. These results are particularly suggestive because a higher cladosporol-mediated inhibition of cell proliferation, as observed in PC-3 cells (see Fig. 1), well correlated with a higher expression of the PPARγ

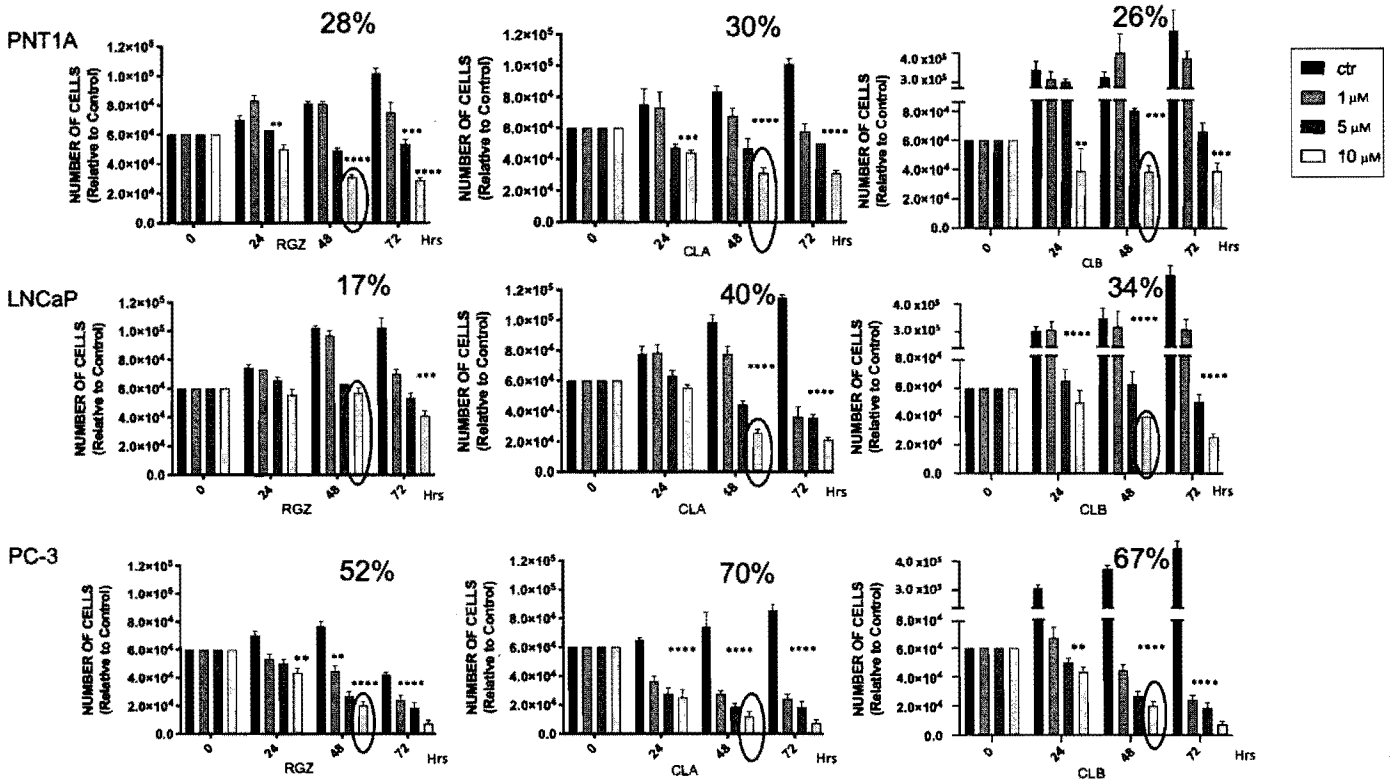

Fig. 1. Cladosporols A and B differentially inhibited the growth of the human PNT1-A, LNCaP and PC-3 prostate cell lines. To evaluate the effect of both cladosporols and rosiglitazone on PNT-1A, LNCaP and PC-3 proliferation, the cells were treated or not with 1, 5 and 10 μM of rosiglitazone, cladosporol A and cladosporol B for 24, 48 and 72 hrs, collected and counted. The data shown here are the mean ± SD of three experiments performed in triplicate. The results were similar in three independent experiments. ** $p < 0.01$, *** $p < 0.001$ and **** $p < 0.0001$ compared to the control (black bar), the untreated cells. 0 in the graph represents the initial time at which the cells were seeded at the same density. For a better understanding of the data, the percentage numbers, above each graph, referring to the underlying bar enclosed in the oval, are reported. These numbers indicate, as an example, the inhibition percentage for PNT-1A, LNCaP and PC-3, respectively, after the administration of 10 μM cladosporol A or B or rosiglitazone (RGZ) for 48 hrs.

receptor in the same type of prostate cells.

To definitively verify whether cladosporols A and B were able to inhibit human prostate cancer cell proliferation through the involvement of PPARγ, we pretreated PNT-1A, LNCaP and PC-3 cells with 5 μM GW9662, the well-known antagonist and irreversible inhibitor of PPARγ, and then exposed the same cells to cladosporols A and B 10 μM for 48 hrs. Cell extracts were analyzed, by western blotting analysis, to evaluate PPARγ expression. A visible decrease of PPARγ isoform 2 expression, following the cladosporol A and B treatments in PC-3 cell line, has been demonstrated (Fig. 4**A**). Notably, a further reduction of PPARγ2 isoform expression was found when the cells were pretreated with GW9662, thus confirming that PPARγ2 was the target of both cladosporols, while PPARγ1 appeared not fully affected by GW9662 modulation (Fig. 4**B and C**). These data clearly indicated that also in human prostate cells cladosporols A and B acted as a specific PPARγ ligand, thus promoting cell growth inhibition.

To further demonstrate that modulation of cell proliferation was PPARγ-dependent, we overexpressed PPARγ in PNT-1A cells (Fig. 4**D**), in which we found lower levels of PPARγ expression (see Fig. 3A), and specifically silenced this receptor in PC-3 cells (Fig. 4**F**), in which PPARγ was expressed at higher levels (see Fig. 3A). The overexpression of PPARγ in cladosporol-treated PNT-1A cells caused, as expected, a reduction of proliferation, as demonstrated by CCK-8 assay (Fig. 4**E**). On the contrary, PPARγ knock-down in PC-3 cells provoked an increase of cell growth (Fig. 4**G**). These results, finally, confirmed the involvement of PPARγ in the cladosporol-mediated regulation of prostate cell proliferation.

3.3. The PPARγ mediated inhibition of the growth of cladosporol-treated human prostate cancer cells was associated with an increase of apoptosis

We decided to deeply investigate the mechanisms through which cladosporols A and B caused the PPARγ-mediated inhibition of PC-3 prostate cancer cell growth. To this aim, we treated PC-3 cells for 48 hrs with both drugs, stained with Annexin V-FITC/propidium iodide and analyzed for modifications in PC-3 membrane structures by flow cytometry. As reported in Fig. 5**A–C**, treatment with 10 μM of cladosporols A and B induced an increase in pre-apoptotic and apoptotic PC-3 cells when compared to the control. The effect was further evident after treatment with 20 μM of both drugs. In the same experiment, we also evaluated the number of necrotic cells following treatment with different doses of cladosporols. These numbers did not significantly change ruling out necrosis as an alternative mode of cell death induced by cladosporols. The decreased expression of well-known apoptotic markers (caspase-3, Bcl-2 and caspase-9) and the increase of cleaved caspase-3, analyzed by western blotting, confirmed the effects of cladosporols on PC-3 cells (Fig. 5**D–J**).

3.4. Cladosporols A and B influenced the proliferation and migration of PC-3 cells

To quantitatively and qualitatively verify the inhibitory activity of cell proliferation and migration mediated by cladosporol treatment on PC-3 cells, a wound healing assay was performed. Cells were treated with two different concentrations of cladosporols A and B (10 and 20 μM) and images were captured at 0, 48 and 72 hrs, after wound formation. Images of Fig. 6A demonstrated that treatment of PC-3 cells with

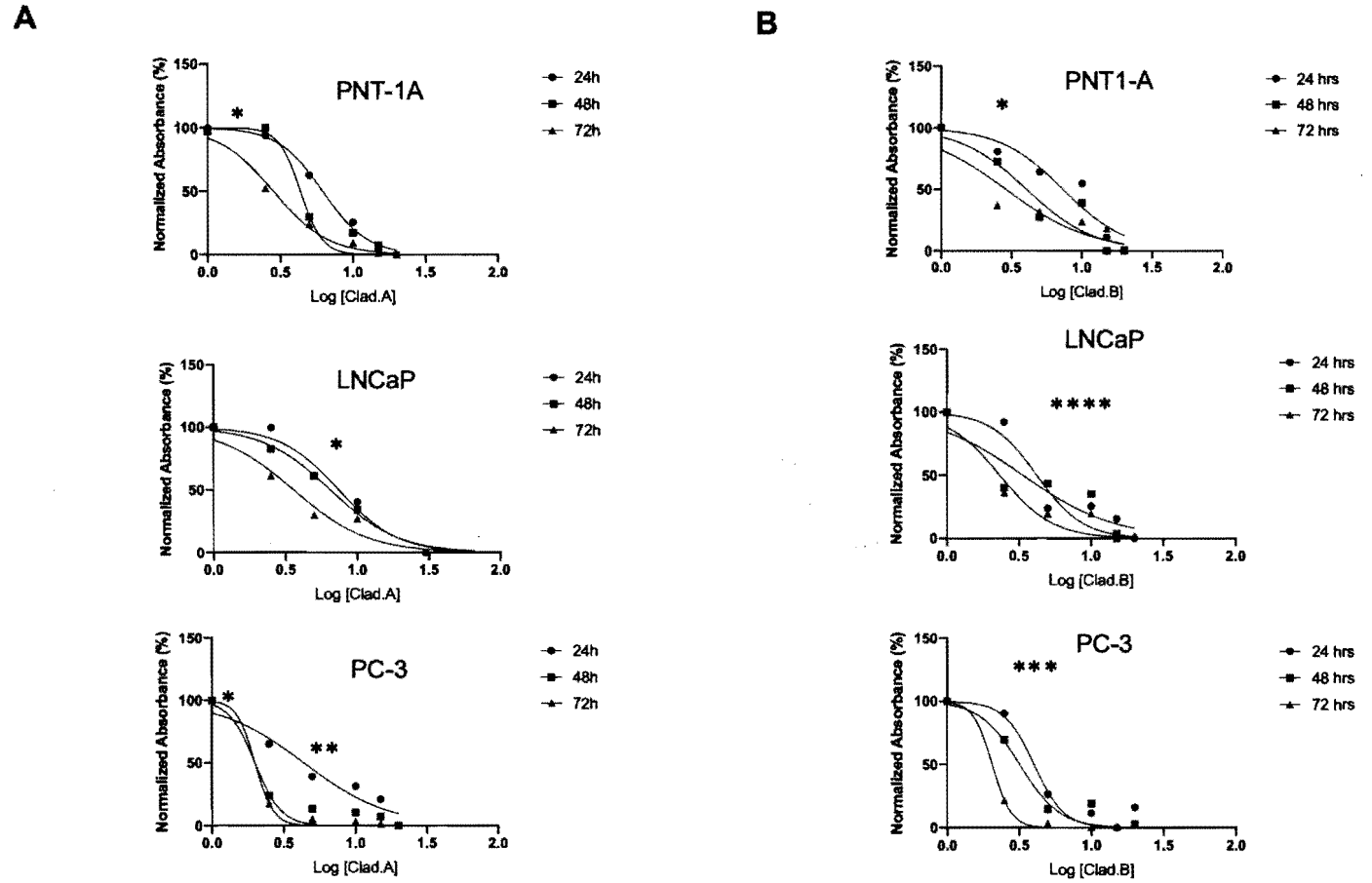

Fig. 2. Cytotoxicity analysis after treatment with cladosporols A and cladosporol B of PNT1-A, LNCaP and PC-3 prostate cells. The dose-dependent cytotoxicity in prostate cells was determined using the CCK-8 cell count assay to evaluate IC_{50} values. PNT-1A, LNCaP and PC-3 cells were seeded in 96-well plates to achieve cell density/cm2 under standard conditions at density of $5x10^3$ cells/cm^2. After 24 hrs, cells were exposed to increasing concentrations of cladosporol A (Fig. 2A) and cladosporol B (Fig. 2B) (2.5 to 20 μM) and growth was evaluated for 24, 48 and 72 hrs by using CCK-8 reagent that was added to vital cells in the plate, following the protocol explained in Materials and Methods Section. Absorbance was measured at 450 nm and IC_{50} values, relative to prostate cancer cells treated with cladosporol A and cladosporol B, were found. For Fig. 2A *p < 0.05 **p < 0.01 compared to the control. For Fig. 2B *p < 0.05 ***p < 0.001 ****p < 0.0001 compared to the control.

Table 1
IC_{50} values relative to prostate cancer cells treated with cladosporol A were reported. The data represent the mean ± SEM of three independent experiments and were expressed as the absorbance ratio of the difference between treated and untreated cells.

	PNT-1	LNCaP	PC-3
24 Hrs	6.54 ± 0.34 μM	7.91 ± 0.40 μM	4.75 ± 0.35 μM
48 Hrs	5.10 ± 1.89 μM	6.22 ± 2.80 μM	3.87 ± 0.72 μM
72 Hrs	3.67 ± 2.02 μM	3.93 ± 0.34 μM	2.52 ± 0.58 μM

Table 2
IC_{50} values relative to prostate cancer cells treated with cladosporol B were reported. The data represent the mean ± SEM of three independent experiments and were expressed as the absorbance ratio of the difference between treated and untreated cells.

	PNT-1	LNCaP	PC-3
24 Hrs	7.14 ± 0.20 μM	3.98 ± 0.23 μM	4.01 ± 0.01 μM
48 Hrs	4.25 ± 0.20 μM	3.26 ± 0.11 μM	3.03 ± 0.16 μM
72 Hrs	3.39 ± 0.52 μM	2.60 ± 0.36 μM	2.07 ± 0.02 μM

both cladosporols, for 48 and even for 72 hrs, was responsible for a reduced capability of the cells in proliferating and migrating. The quantitative evaluation, reported in Fig. 6**B and C**, confirmed the antiproliferative effects of cladosporols. Modulation of the expression of proteins involved in cell proliferation and migration (β -catenin, E-cadherin, MMP-9), observed by Western blotting analysis, proved the inhibitory function of cladosporols A and B (Fig. 6**D–H**).

Adipose tissue usually influences the tumor microenvironment through the exchange of regulatory factors and metabolic substrates. We have already demonstrated that secreted factors from cladosporol-treated 3 T3-L1 cells were able to regulate HT-29 cell growth and migration and, therefore, we wanted to investigate the same effects on prostate cell proliferation [17]. To achieve this, we allowed 3T3-L1 preadipocytes to differentiate and collected the medium from cells treated with MDI, MDI plus 5 μM rosiglitazone or 5 μM cladosporol A or 5 μM cladosporol B, respectively. We filtered the medium and used it as conditioned medium to analyze the effect on PC-3 cell proliferation and migration. To determine the effects of the 3T3-L1-conditioned medium on PC-3 cell migration, we carried out a wound healing assay as above described and captured images at 0, 48 and 72 hrs after wound formation to evaluate the degree of healing. Conditioned medium from 3T3-L1 preadipocytes, differentiated adipocytes (treated with MDI) and treated with MDI plus RGZ promoted the migratory ability of PC-3 prostate cells (Fig. 7**B**). On the contrary, the migration of PC-3 cells was significantly arrested after exposure to conditioned medium collected from 3T3-L1 cells treated with MDI plus cladosporol A or cladosporol B (Fig. 7**B**). The quantitative evaluation of these effects was reported in Fig. 7**C and D**. These effects on proliferation and migration of the same cell type

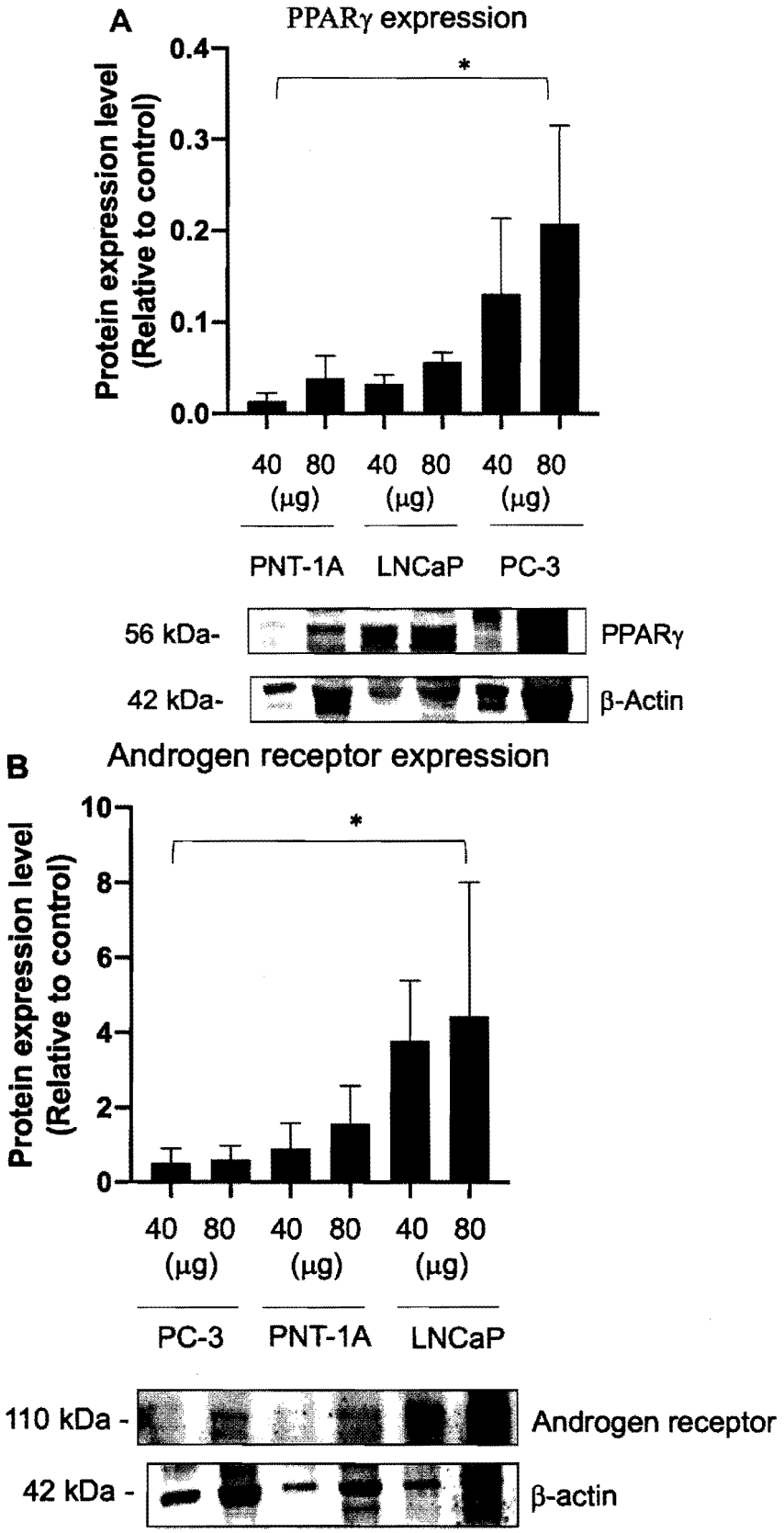

Fig. 3. Prostate-derived cells differentially expressed PPARγ and androgen receptor proteins. Western blotting analysis of PPARγ (A) and androgen receptor (B) expression level on increasing dosages of total protein extracts (40 and 80 μg) from PNT-1A, LNCaP and PC-3 prostate cells. Normalization of the loaded samples was performed using an anti-β-actin antibody. The western blotting shown here is only a representative experiment. The bar graphs represent the mean ± SD of protein/β-actin of at least three independent experiments. * $p < 0.05$ compared to the control.

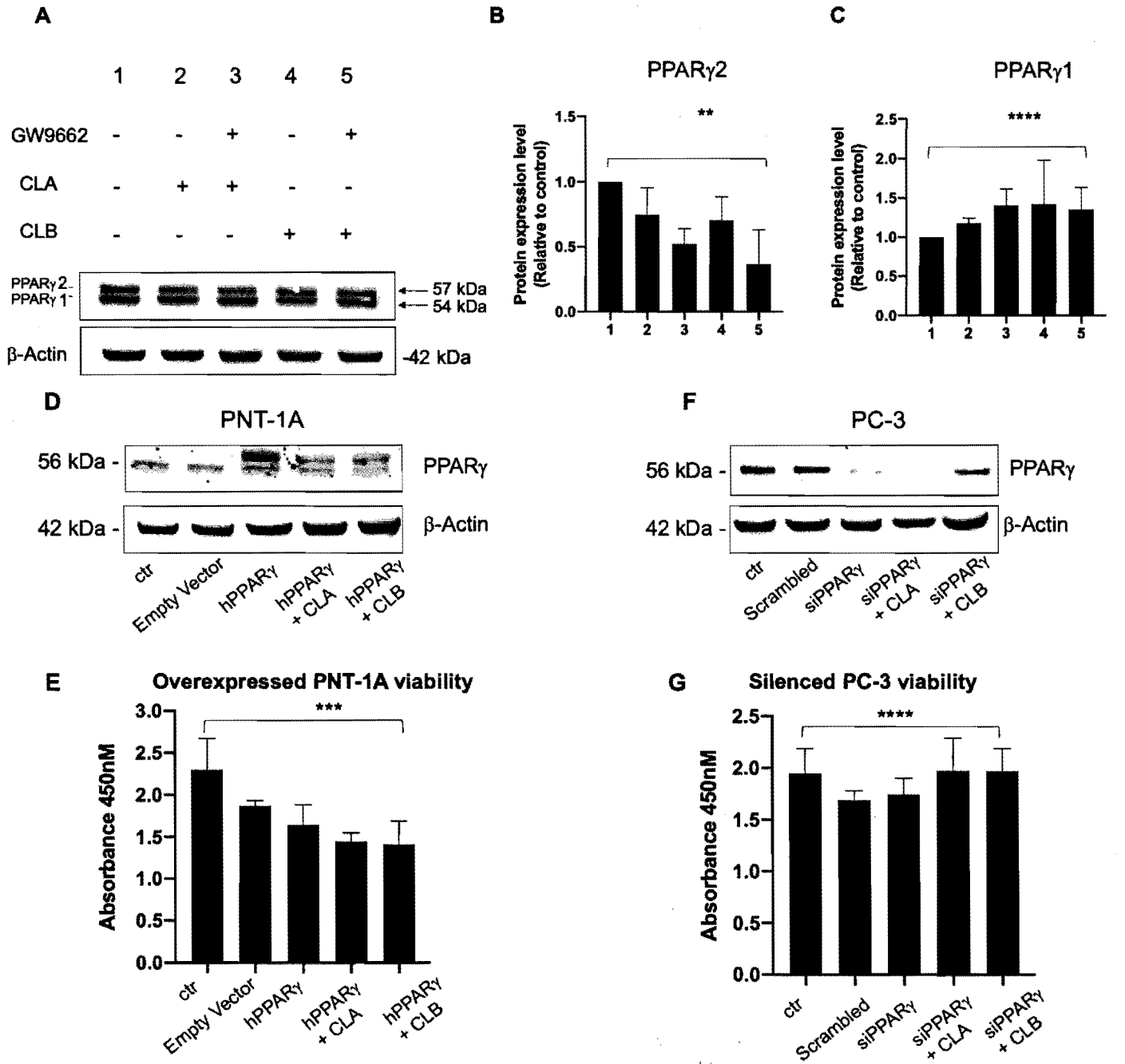

Fig. 4. Antiproliferative activity of cladosporols A and B is mediated by PPARγ. (A) Western blotting analysis of PPARγ on extracts from PC-3 cells pretreated or not with 5 μM GW9662 and then treated with 10 μM cladosporol A and cladosporol B for 48 hrs. Normalization of the loaded samples was performed using an anti-β-actin antibody. The western blotting shown here is only a representative experiment. (B, C) The bar graphs represent the mean ± SD of at least three independent experiments. **p < 0.01 ****p < 0.0001 compared to the control. Western blotting analysis on extracts from PNT-1A cells (D), in which PPARγ was overexpressed and on extracts from PC-3 cells (F), in which PPARγ was silenced, is shown. Cell viability was evaluated on PNT-1A cells (E) and on PC-3 cells (G) using the CCK-8 cell count assay and absorbance was measured at 450 nm as described in Fig. 2. The bar graphs represent the mean ± SD of at least three independent experiments. ***p < 0.001 ****p < 0.0001 compared to the control.

appeared to be stronger than that shown in Fig. 6A. We also modified the protocol, as indicated in Materials and Methods section (see also scheme in Fig. 7A), collecting the conditioned medium from 3T3-L1 cells exposed to MDI plus cladosporol A or cladosporol B after deprivation of both drugs during the last two days of cell differentiation (the new samples are indicated as MDI-CLA and MDI-CLB in Fig. 7A). We changed this protocol to clarify that the inhibition of cell migration was due to the effects of cladosporols on 3T3-L1 adipocyte differentiation and not directly to the presence of the drugs in the conditioned medium. In these new experimental conditions, the conditioned medium designed as MDI-CLA and MDI-CLB also caused inhibition of PC-3 cell migration (Fig. 7B–D). The inhibitory effect was strongly confirmed by western blotting analysis shown in Fig. 8A–K. A decreased expression of β -catenin, cyclin D1, caspase-3 and MMP-9 well correlated to an increased amount of E-cadherin and cleaved caspase-3 in PC-3 prostate cells treated with the medium derived from 3T3-L1 cells treated with MDI plus cladosporol A or cladosporol B. Note also that in this latter experiment we used doses of cladosporols on 3T3-L1 cells lower than the ones

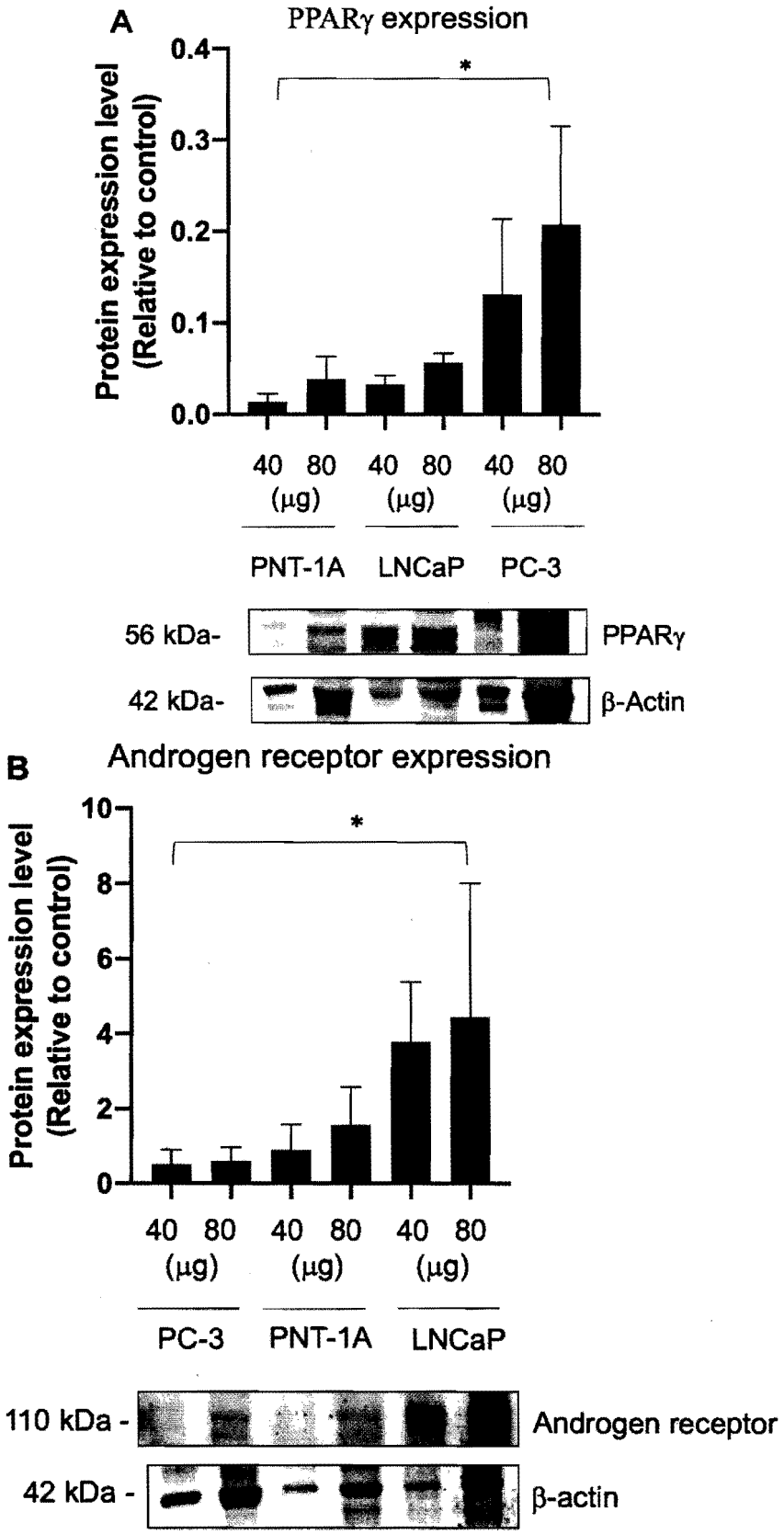

Fig. 3. Prostate-derived cells differentially expressed PPARγ and androgen receptor proteins. Western blotting analysis of PPARγ (A) and androgen receptor (B) expression level on increasing dosages of total protein extracts (40 and 80 μg) from PNT-1A, LNCaP and PC-3 prostate cells. Normalization of the loaded samples was performed using an anti-β-actin antibody. The western blotting shown here is only a representative experiment. The bar graphs represent the mean ± SD of protein/β-actin of at least three independent experiments. * $p < 0.05$ compared to the control.

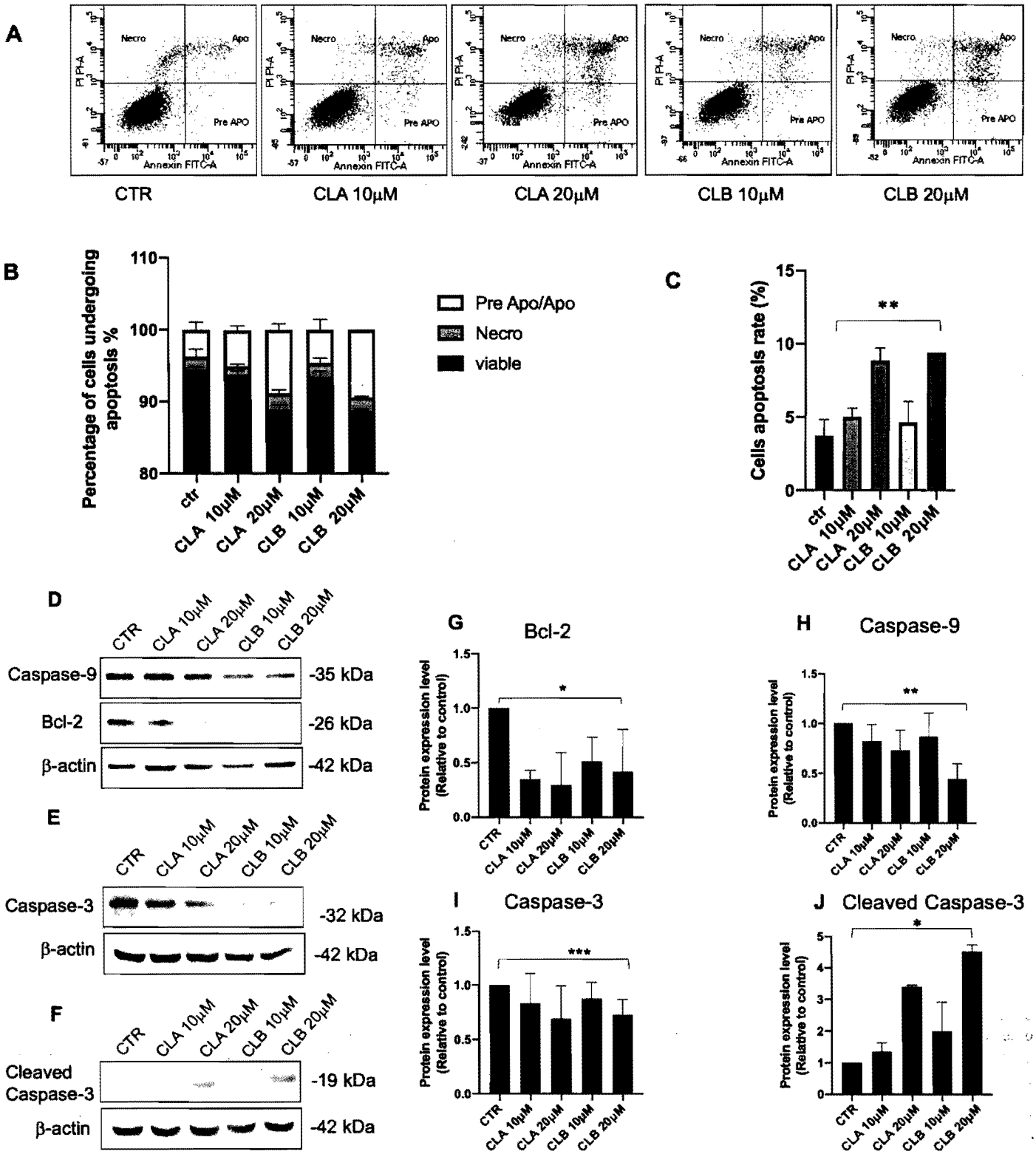

Fig. 5. Cladosporol A and B stimulated apoptosis of human PC-3 prostate cancer cells. (A) Flow cytometric analysis of membrane alterations in PC-3 prostate cancer cells treated for 48 hrs with the indicated doses (10 and 20 μM) of cladosporol A and cladosporol B, respectively, followed by Annexin V-propidium iodide staining. (B) Necrotic and preapo/apoptotic cells were evaluated in percentages versus viable cells and reported in the graphic representations. (C) Apoptosis rate in percentage in the PC-3 population treated for 48 hrs with both cladosporols (10 and 20 μM) compared to the untreated cells (ctr, control). The bar graphs represent the mean ± SD of at least three independent experiments. $^{**}p < 0.01$ compared to the control. (D) Western blotting analysis of the expression of specific apoptotic markers (Bcl-2 and caspase 9), (E) (caspase 3) and (F) (cleaved caspase-3) on extracts from PC-3 prostate cancer cells treated with 10 and 20 μM cladosporol A and cladosporol B for 48 hrs. Normalization of the loaded samples was performed using an anti-β-actin antibody. The western blotting shown here is only a representative experiment. (G-J) The bar graphs represent the mean ± SD of protein/β-actin of at least three independent experiments. $^{*}p < 0.05$ $^{**}p < 0.01$ $^{***}p < 0.001$ compared to the control.

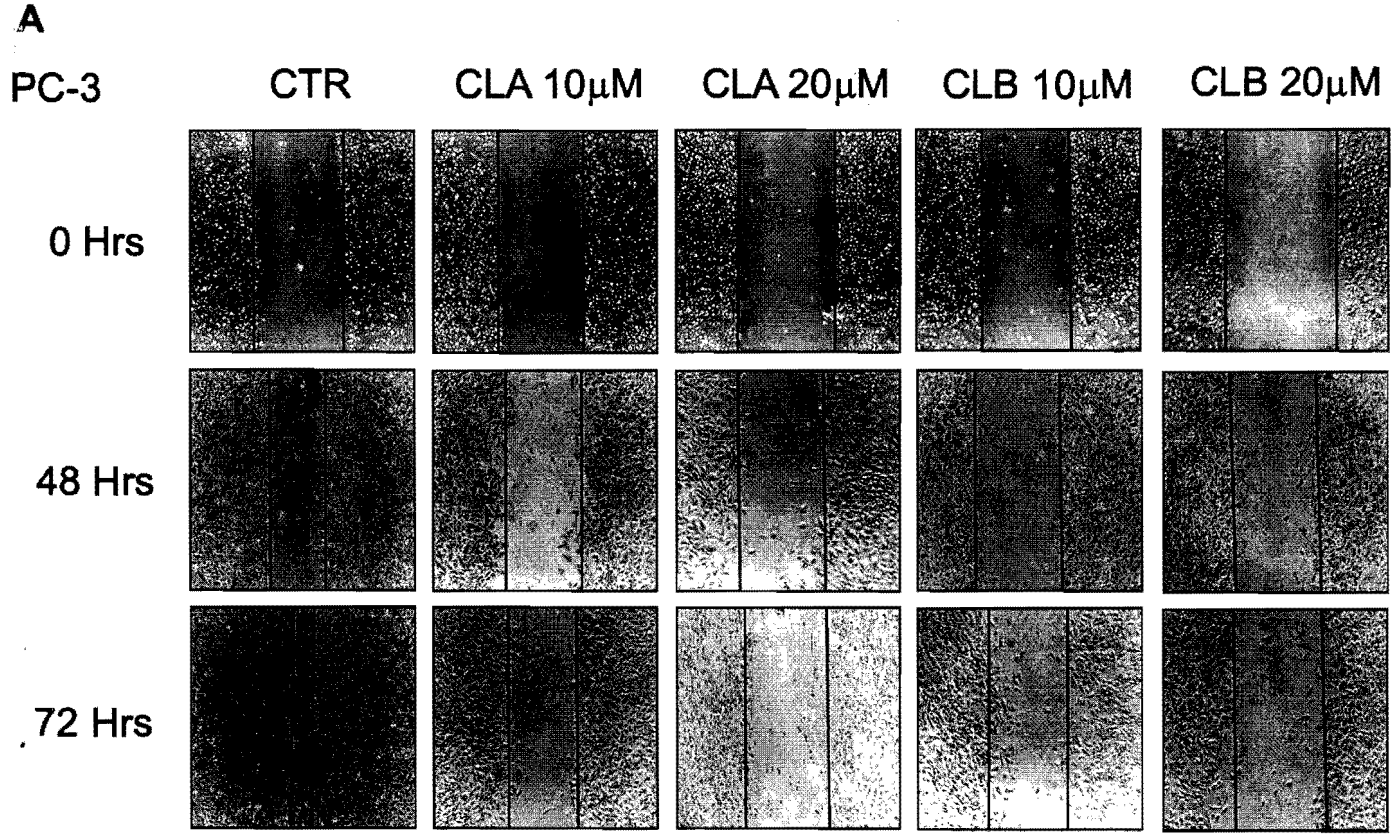

Fig. 6. Cladosporols A and B inhibited PC-3 metastatic prostate cancer cell proliferation and migration. (A) Cells were plated at a subconfluent density (8.0×10^4 cells/ml) in growth medium. Once they reached 100 % confluence, a wound was formed using the 10 μL plastic micropipette tip. Afterwards, cells were treated for 48 and 72 hrs with two different doses of cladosporols A and B (10 and 20 μM). (B) In the table are reported the measurements of the closure (indicated in μm) of the scratch executed on the PC-3 prostate cancer cells and successively treated for 48 and 72 hrs with two different doses of cladosporol A and B (10 and 20 μM). Data are represented as the mean ± SEM of three independent experiments. (C) In the graph is reported the evaluation of wound closure (in percentage) after treatment of the PC-3 prostate cancer cells with two different doses of cladosporol A and B (10 and 20 μM) for 48 and 72 hrs..***$p < 0.001$ ****$p < 0.0001$ compared to the control. (D) Western blotting analysis of the expression of specific markers of cell migration (β -catenin and E-cadherin) on the total extracts from PC-3 cells treated with 10 and 20 μM cladosporol A and cladosporol B for 48 hrs. (E) Western blotting analysis of MMP-9 expression on the total extracts from PC-3 cells treated with 10 and 20 μM cladosporol A and cladosporol B for 48 hrs. Normalization of the loaded samples was performed using an anti-β-actin antibody. The western blotting shown here is only a representative experiment. (F-H) The bar graphs represent the mean ± SD of protein/β-actin of at least three independent experiments. ***$p < 0.001$ ****$p < 0.0001$ compared to the control.

used on PC-3 cells of the Fig. 6 (5 μM versus 10 or 20 μM). It is reasonable, indeed, to assume that treatment of 3T3-L1 cells with cladosporols could cause secretion of protein factors from adipocytes that influenced PC-3 cell proliferation and migration. The increase of adiponectin receptor 1 (Adipo-R1) expression in PC-3 cells cultured in the cladosporol-conditioned medium (Fig. 8I) is, therefore, consistent with the presence of higher adiponectin protein levels in the medium (Fig. 8M) compared to those of leptin (Fig. 8L). It is noteworthy that the inhibitory effects on PC-3 metastatic cells were higher than the ones revealed in PNT-1A cells (compare Fig. 7**E with** Fig. 7**B**) as demonstrated also by the quantitative evaluation reported in Fig. 7**D** and **G**. Altogether, these results confirmed that PC-3 cells, showing a higher sensitivity to both cladosporols in terms of cell viability (**see** Figs. 1–2), displayed also a sensible responsiveness in terms of motility inhibition.

3.5. Inhibition of the growth of human prostate cancer cells due to cladosporols A and B was correlated to dysregulated lipid metabolism

In prostate cancer cells a higher *de novo* lipogenesis is a critical condition for sustaining an increased demand of lipids to permit membrane construction, energy storage, redox balance and activation of intracellular pathways [33]. We decided to verify whether cladosporols also displayed a regulatory function in lipid metabolism in prostate cells. To this aim, we treated PNT-1A, LNCaP and PC-3 cells with cladosporol A or cladosporol B, respectively, and then stained them with Oil Red O. All the cellular types were able to accumulate lipids with the PC-3 cells showing their highest storage ability (compare the optical microscope fields and the images of plate controls in A and B of the Fig. 9). Treatment of PNT-1A, LNCaP and PC-3 cells with cladosporols dramatically inhibited lipid accumulation (see the evaluation reported in the graph of Fig. 9**C**). It is very interesting that, in the most advanced and metastatic PC-3 cancer cells, the strong ability to accumulate lipids correlated with the aggressiveness of cancer and was efficiently counteracted by cladosporol treatment. Since aggressive prostate cancer promotion is independent on extracellular or circulating lipids and requires an endogeneous lipid synthesis [18–20], we investigated whether cladosporol A or cladosporol B inhibited lipid storage in PC-3 cells through a negative regulation of their synthesis. Indeed, we analyzed, by western blotting, the expression of some enzymes directly involved in the lipid metabolism (sterol responsive element binding protein 1, SREBP-1; hydroxi-methyl-glutaril-CoenzymeA reductase, HMG-CoAr; acetyl-CoenzymeA carboxilase, ACC; fatty acid binding protein 4, FABP4; fatty acid synthase, FAS). The results of Fig. 10A–I indicated that, at steady state, the protein levels of these enzymes were overall reduced by

B

Wound quantification

PC-3	CTR	CLA 10μM	CLA 20μM	CLB 10μM	CLB 20μM
0 Hrs	866± 1.2 (μm)	844.7± 19.9 (μm)	866.3± 76.4 (μm)	901± 20.9 (μm)	844.3± 58.6 (μm)
48 Hrs	592± 38.5 (μm)	759.3± 0.4 (μm)	742.3± 96.7 (μm)	726.3± 20.4 (μm)	721.7± 43.9 (μm)
72 Hrs	354.6± 82.5 (μm)	596.3± 0.4 (μm)	647.7± 76.8 (μm)	648± 2.4 (μm)	671± 58.2 (μm)

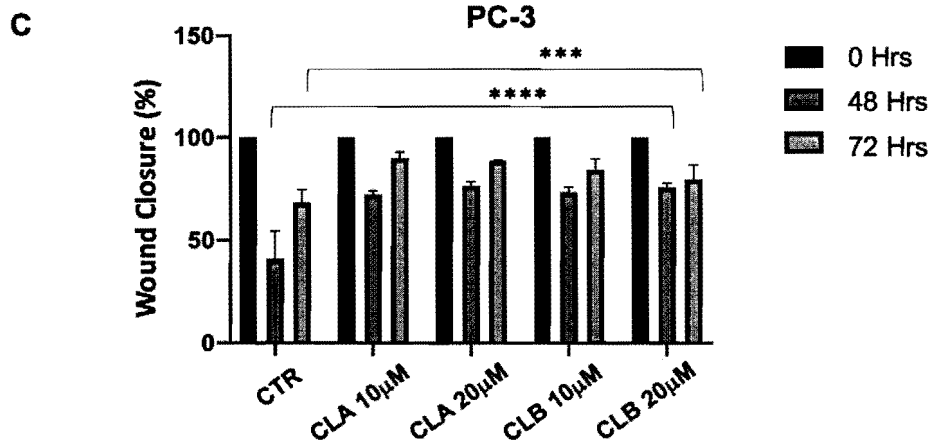

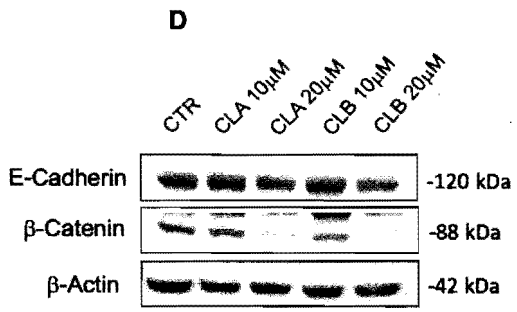

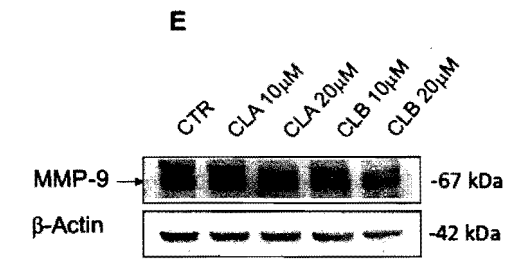

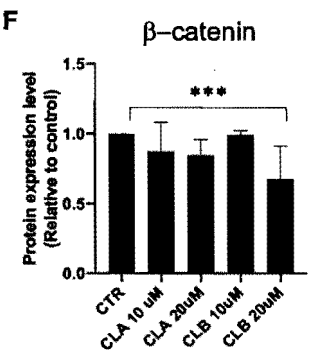

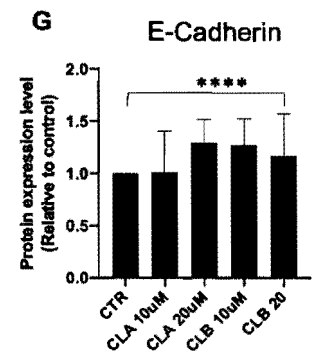

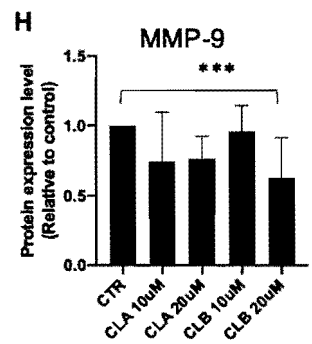

Fig. 6. (*continued*).

cladosporol treatments. As expected, the pretreatment with GW9662 provoked a further reduction confirming that the negative regulatory effect on the lipid *de novo* synthesis was dependent on binding of cladosporols to the PPARγ LBD.

4. Discussion

Prostate cancer, a multifaceted disease, strictly depends on different risk factors (age, race, diet, smoking, physical activity, genetic alterations and inflammation). While genetic mutations account for about 10% of the causes of prostate cancer, epigenetic modifications due to environmental conditions or lifestyle contribute to the remaining 90%

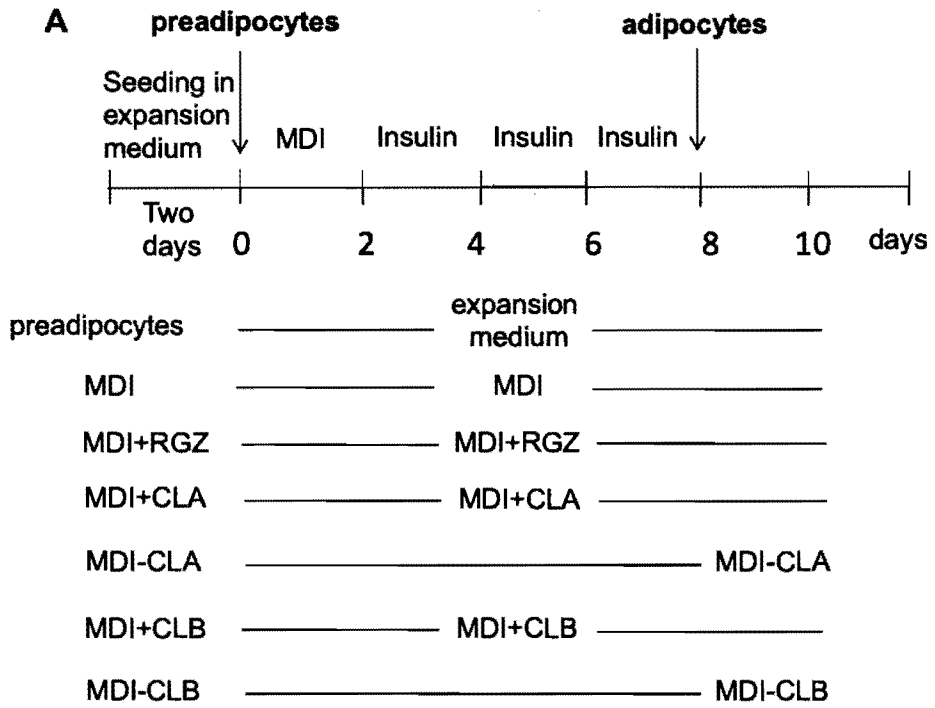

Fig. 7. Conditioned medium from 3 T3-L1 cells treated with cladosporol A or cladosporol B inhibited PC-3 cell migration and invasion. (A) Scheme describing the 3T3-L1 preadipocyte differentiation and cladosporol treatment protocols followed for the migration assay shown below. 3T3-L1 preadipocytes were differentiated and the medium from cells treated, respectively, with MDI, MDI plus 5 μM rosiglitazone (MDI + RGZ) or MDI plus 5 μM cladosporol A (MDI + CL A) or MDI plus 5 μM cladosporol B (MDI + CL B) was collected. In addition, other two medium samples were prepared collecting the medium from 3T3-L1 cells treated with MDI plus CL A and CL B, but deprived of both drugs in the last two days of cell differentiation (the new samples are indicated as MDI-CL A and MDI-CL B). (B) The wound healing assay was carried out, as described above for Fig. 6A, but the conditioned medium from 3T3-L1 cells was used to culture PC-3 cells for 24, 48 and 72 hrs. Cells were plated at a subconfluent density (8.0×10^4 cells/ml) in growth medium. Once they reached 100 % confluence, a wound was formed using the 10 μL plastic micropipette tip. (C) In the table are reported the measurements of the closure (indicated in μm) of the scratch executed on the PC-3 prostate cancer cells and successively exposed for 48 and 72 hrs to the conditioned medium from undifferentianted 3T3-L1 cells (Pre-3T3-L1), 3T3-L1 cells treated with differentiation mix MDI, MDI plus 5 μM rosiglitazone (MDI + RGZ) or MDI plus 5 μM cladosporol A (MDI + CLA) or (MDI - CLA) or MDI plus 5 μM cladosporol B (MDI + CL B) or MDI-CLB. Data are represented as the mean ± SEM of three independent experiments. (D) In the graph is reported the evaluation of wound closure (in percentage) of the scratch executed on the PC-3 prostate cancer cells and successively exposed for 48 and 72 hrs to the conditioned medium from undifferentianted 3T3-L1 cells or 3T3-L1 cells treated with differentiation mix MDI or MDI plus 5 μM rosiglitazone (MDI + RGZ) or MDI plus 5 μM cladosporol A (MDI + CLA) or (MDI - CLA) or MDI plus 5 μM cladosporol B (MDI + CL B) or MDI- CLB. ****$p < 0.0001$ compared to the control. (E) The same wound healing assay was carried out on PNT1-A. (F) In the table are reported the measurements of the closure (indicated in μm) of the scratch executed on the PNT1-A prostate cells and successively exposed for 48 and 72 hrs to the conditioned medium from undifferentianted 3T3-L1 cells (Pre-3T3-L1) or 3T3-L1 cells treated with differentiation mix MDI or MDI plus 5 μM rosiglitazone (MDI + RGZ) or MDI plus 5 μM cladosporol A (MDI + CLA) or (MDI - CLA) or MDI plus 5 μM cladosporol B (MDI + CL B) or MDI- CLB. Data are represented as the mean ± SEM of three independent experiments. (G) In the graph is reported the evaluation of wound closure (in percentage) of the scratch executed on the PNT1-A prostate cells and successively exposed for 48 and 72 hrs to the conditioned medium from undifferentianted 3T3-L1 cells (Pre-3T3-L1) or 3T3-L1 cells treated with differentiation mix MDI or MDI plus 5 μM rosiglitazone (MDI + RGZ) or MDI plus 5 μM cladosporol A (MDI + CLA) or (MDI - CLA) or MDI plus 5 μM cladosporol B (MDI + CL B) or MDI- CLB. Data are represented as the mean ± SEM of three independent experiments. ****$p < 0.0001$ compared to the control.

[34]. Given the complexity of this disease, it is essential to diagnose cancer prostate early to therapeutically manage patients and prevent mortality. To better diagnose prostate cancer, Prostate Specific Antigen (PSA) evaluation, Digital Rectal Examination (DRE), prostate biopsy, and multiparametric Magnetic Resonance Imaging (MRI) are helpful. It is noteworthy that patients affected by prostate cancer are usually asymptomatic and that their disease may be fully diagnosed only after 65 years. Indeed, men do not show clear symptoms until the onset of the disease and a symptom may often be shared with benign prostate hyperplasia [35,36]. One of the most relevant risk factors associated with prostate cancer is the influence of endogenous hormones and, particularly, androgens, which are recognized as responsible for the proliferation and differentiation of the luminal epithelium of the prostate and as causative agents of the initiation and progression of cancer [37]. Based on these data, the treatment protocols for managing prostate cancer patients consisted of androgen deprivation. Inhibition of androgen stimulation provoked a partial or full remission in several cases, but, successively, the reappearance of the disease in a much more aggressive and totally androgen-independent form, prompted researchers to look for other putative targets and alternative therapeutical approaches [38].

More recently, PPARγ became an exciting study object with the aim of better revealing its features and using it as a new molecular target in the development of improved antitumor strategies for androgen-independent prostate cancer. From PPARγ gene, through the use of four major transcription initiation sites, four mature mRNAs are generated [22]. Three of these mRNAs (PPARγ 1, 3 and 4) produce the same PPARγ1 protein, whereas the messenger of PPARγ2, through its translation, leads to the formation of PPARγ2 protein, which includes a further 28 amino acids at the N-terminus. Both PPARγ1 and PPARγ2 isoforms, sharing the same structure, have a cell-specific expression pattern. PPARγ1 is expressed at relatively high levels in different tissues and in numerous cells of the immune system. PPARγ2 expression, instead, is mostly expressed in adipose tissue, where it acts as one of the major transcription factors in adipogenesis. PPARγ2 promotes the *in vitro* differentiation of adipocytes, while *in vivo* it reduces circulating non-esterified fatty acids (NEFA) and improves insulin sensitivity [39].

B

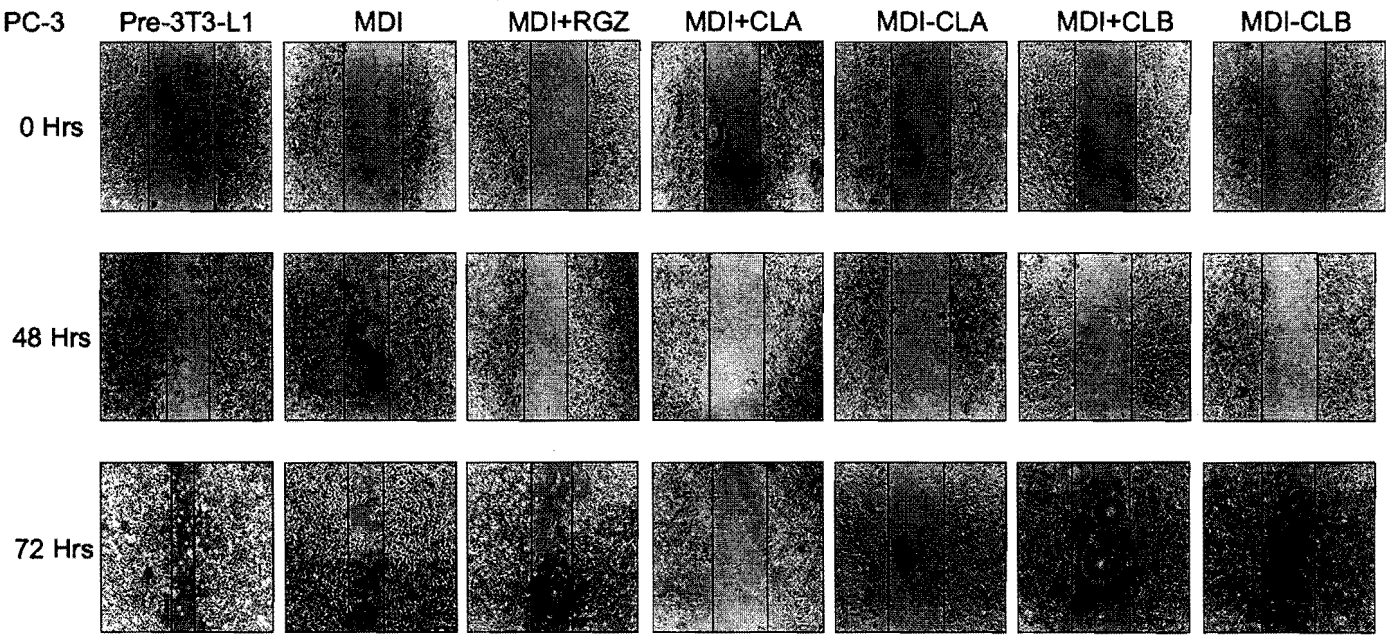

C

Wound quantification

PC-3	Pre-3T3-L1	MDI	MDI+RGZ	MDI+CLA	MDI-CLA	MDI+CLB	MDI-CLB
0 Hrs	811.3± 2 (μm)	749.6± 11 (μm)	723.3± 58.5 (μm)	791.3± 58.1 (μm)	773.6± 42.8 (μm)	791.7± 20 (μm)	754± 33.7 (μm)
48 Hrs	529± 41.3 (μm)	540.5± 1.6 (μm)	574.3± 20 (μm)	754± 63.9 (μm)	718± 53.7 (μm)	700± 71.1 (μm)	644.7± 97 (μm)
72 Hrs	343± 58 (μm)	461.6± 19 (μm)	517± 19.2 (μm)	724± 43.4 (μm)	646± 124.3 (μm)	634± 124 (μm)	607± 140.6 (μm)

D

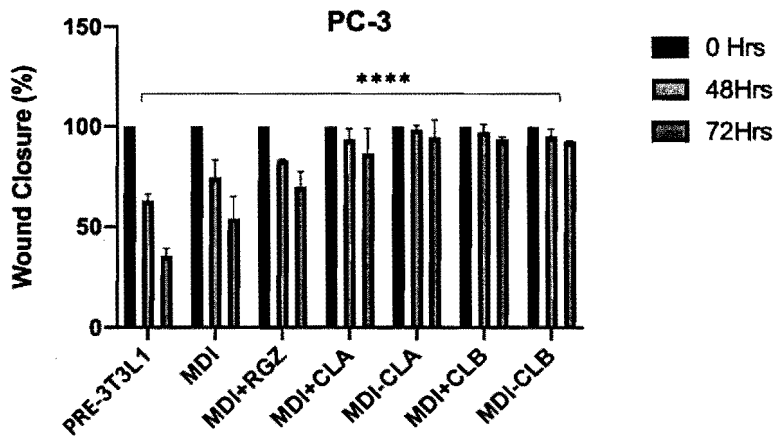

Fig. 7. (*continued*).

We have largely demonstrated that PPARγ is the molecular target of cladosporols, secondary metabolites of *Cladosporium tenuissimum*, displaying antiproliferative and proapoptotic activities towards colon cancer cells [14–16]. We here extended these observations in prostate cancer cells, as demonstrated by the results of Figs. 1 and 2. In particular, we demonstrated that cladosporols A and B inhibited proliferation of the three types of prostate cells, but the greatest inhibitory effects were obtained against the most aggressive and metastatic PC-3 cells. This selective ability of cladosporols towards PC-3 cells is very interesting, considering that too many drugs used in the anticancer therapy show disastrous effects on normal cells. Indeed, it is hopeful to have available specific anticancer drugs that are able to target late-stage cancer cells without side effects.

To investigate the mechanisms responsible of sensitivity to cladosporol treatment of metastatic PC-3 prostate cells, we evaluated the expression of PPARγ in PC-3 cells compared to PNT-1A and LNCaP cells. The data shown in Fig. 3A indicated a higher PPARγ protein expression in PC-3 cells than that observed in PNT-1A and LNCaP cells. In addition,

E

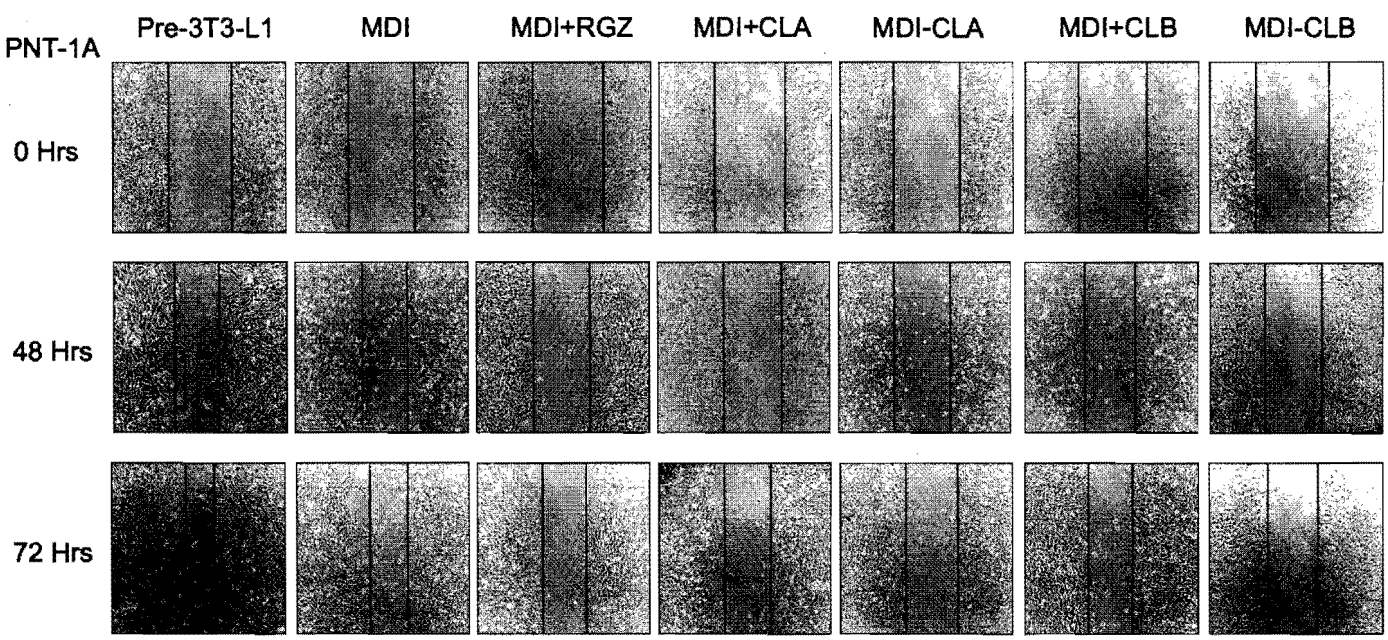

F

Wound quantification

PNT-1A	Pre-3T3-L1	MDI	MDI+RGZ	MDI+CLA	MDI-CLA	MDI+CLB	MDI-CLB
0 Hrs	831 ± 22 (μm)	830.7 ± 44.5 (μm)	831 ± 22 (μm)	886.3 ± 26.8 (μm)	869.3 ± 41.5 (μm)	905 ± 42.9 (μm)	832.3 ± 98.3 (μm)
48 Hrs	596 ± 38.2 (μm)	560 ± 22 (μm)	614 ± 58.3 (μm)	776.3 ± 22.5 (μm)	668 ± 22 (μm)	632 ± 22 (μm)	596 ± 76.4 (μm)
72 Hrs	397.3 ± 22.5 (μm)	451.7 ± 44.5 (μm)	506 ± 44.1 (μm)	668 ± 79.5 (μm)	527.3 ± 78.5 (μm)	488 ± 38.1 (μm)	505.7 ± 96.4 (μm)

G

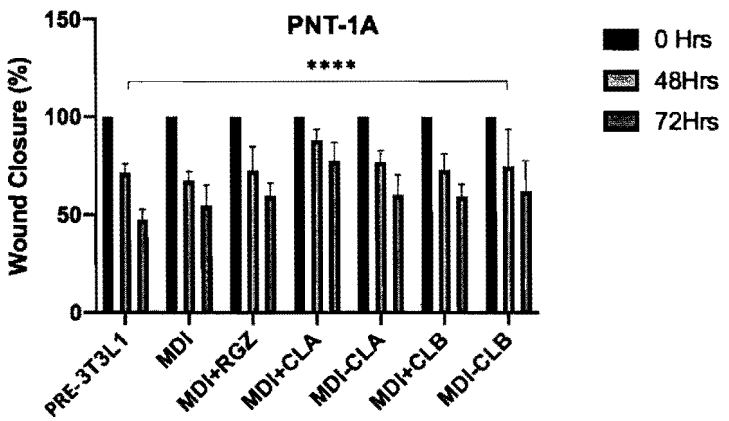

Fig. 7. (*continued*).

the level of PPARγ protein correlated well with the antiproliferative activity of cladosporols in the three prostate cancer-derived cells. As expected, western blotting analysis on the same total protein extracts from PNT-1A, LNCaP and PC-3 cells showed an inverse relationship with AR expression in accordance with previous experimental evidences [40]. Therefore, we verified that AR protein levels were higher in PNT-1A cells than in PC-3 cells (Fig. 3**B**). Variation in AR protein expression is only one of events interfering in its function and AR gene mutation or rearrangements, as well as proteolytic cleavage of full lenght AR, have also been hypothesized as mechanisms for generation of AR variants [41]. These different AR isoforms constitute a feature of tumor samples from patients affected by androgen-independent prostate cancer and their finding suggests that a significant sensitivity of mutated AR could allow a certain sustained response to very low levels of androgen produced autonomously by tumor [42,43]. Starting from the observation of the unequal distribution of PPARγ and AR in the different prostate cancer cells, we decided to analyze whether PPARγ really was the target of the cladosporols in PC-3 cells (Fig. 4**A**). Western blotting analysis of total extracts from these prostate cancer cells indicated that PPARγ2 was coherently modulated by exposure to cladosporols which we have already demonstrated to work as PPARγ inhibitors [14–16]. Moreover, PPARγ2 was further downregulated by treatment with GW9662, an irreversible inhibitor of PPARγ itself, suggesting that cladosporols acted as PPARγ ligands in these cells. As expected, we did not find a significant

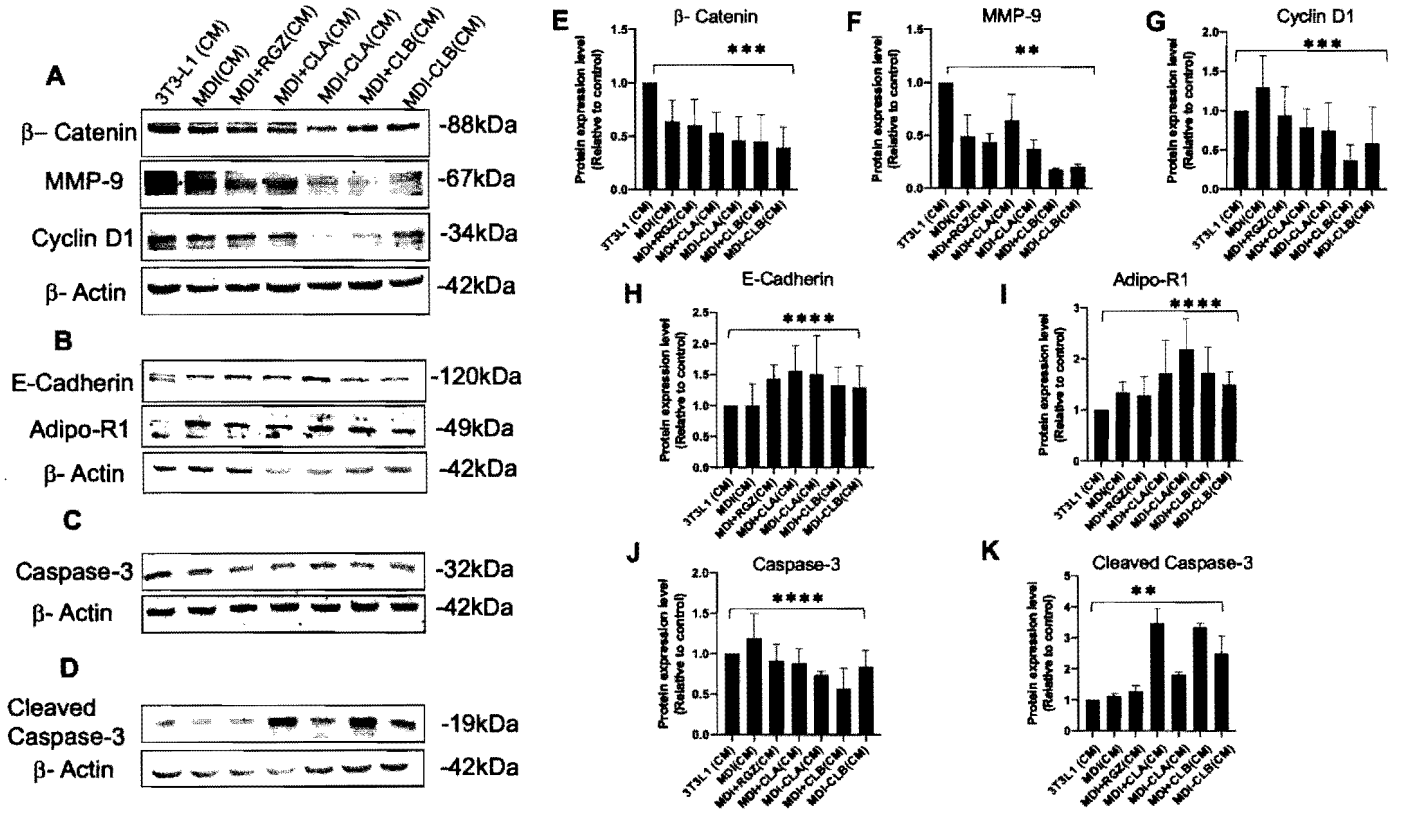

Fig. 8. Modulation of markers involved in PC-3 cell migration, invasion and apoptosis in PC-3 cells cultured with conditioned medium from 3 T3-L1 cells treated with cladosporol A or cladosporol B. (A-D) Western blotting analysis of the expression of β -catenin, MMP-9, Cyclin D1, E-cadherin, Adipo-R1, caspase 3 and cleaved caspase 3 on the total extracts from PC-3 cells treated for 48 hrs with conditioned media from 3T3-L1 cells (MDI, MDI plus 5 μM rosiglitazone (MDI + RGZ), MDI plus 5 μM cladosporol A (MDI + CL A), (MDI-CL A), MDI plus 5 μM cladosporol B (MDI + CL B), (MDI-CL B)). Normalization of the loaded samples was performed using an anti-β-actin antibody. Each panel showing a western blotting is only a representative experiment. (E-K) The bar graphs represent the mean ± SD of a single protein marker/β-actin of at least three independent experiments. $^{**}p < 0.01$ $^{***}p < 0.001$ $^{****}p < 0.0001$ compared to the control. (L-M) 3T3-L1 preadipocytes were differentiated as described in Materials and Methods Section, and the medium from cells treated with differentiation mix MDI, MDI plus 5 μM rosiglitazone (MDI + RGZ) or MDI plus 5 μM cladosporol A (MDI + CL A) or MDI plus 5 μM cladosporol B (MDI + CL B) or MDI-CL A and MDI-CL B was collected. Medium proteins were separated by sodium dodecyl sulfate–polyacrylamide gel electrophoresis and transferred to nylon membranes. Western blotting analysis of secreted leptin and adiponectin protein levels from 3T3-L1 cells was performed. To control the samples loaded and derived from untreated and cladosporol A- and cladosporol B-treated 3T3-L1 cells and normalize the results, a comparison with the protein samples was used after the Ponceau staining. The bar graphs represent the mean ± SD of specific protein/red band of Ponceau of at least three independent experiments. $^{****}p < 0.0001$ compared to the control.

modulation on PPARγ1 expression after these treatments, reinforcing the above results and indicating, at same time, that PPARγ2 played a specific role in controlling the proliferation of PC-3 prostate cancer cells (Fig. 4**A–C**). The PPARγ overexpression and silencing assays of Fig. 4**D–G** confirmed these latter data. PNT-1A cells expressing higher protein levels of total PPARγ and treated with cladosporols displayed a reduced ability to proliferate (see the two last bars in the graph of Fig. 4**E**). These data suggested that to inhibit proliferation in PNT-1A cells, an increase in the PPARγ expression was required. PPARγ knock-down in PC-3 cells (Fig. 4**F**) caused an increase in cell proliferation as shown in the graph of Fig. 4**G**. In other words, a higher PPARγ protein levels were necessary to obtain a strong cladosporol-mediated inhibition of cell proliferation. These results have been confirmed by the work of different laboratories that indicated in the PPARγ2, the longer isoform of this nuclear receptor, the protein displaying a strong proapoptotic and antiproliferative activity in prostate cancer cells. PPARγ1, instead, acts as an oncogene, that is a mediator of increased cell growth [44–47]. Results shown in Fig. 5**A–C** definitively demonstrated that PC-3 cell proliferation decrease is caused by a sustained cell apoptosis. The increase of cleaved caspase-3 and the reduction of caspase-3, Bcl-2 and caspase-9 expression strenghtened this hypothesis (Fig. 5**D–J**).

Metalloproteinases are a homogenous enzyme family involved in the destruction of matrix collagen and basement membrane thus displaying a crucial role in tumor invasion and metastasis [48,49]. Inactivating metalloproteinase action is a potential strategy for inhibiting cancer progression and invasion through the modulation of PPARγ activity. Here, we demonstrated that downregulation of MMP-9 due to cladosporol/PPARγ interaction could be a useful anti-tumorigenic procedure in prostate cancer management. As reported in Fig. 6**D–H**, decreased expression of MMP-9 and β -catenin well correlated with an increase of E-cadherin after cladosporol treatment of PC-3 cells. These results were also in accordance with the ability of both drugs to limit cell migration as shown in Fig. 6**A–C**. A more sustained inhibition of cell proliferation and migration was also obtained by the exposure of PC-3 cells to the conditioned culture media from 3T3-L1 cells treated with cladosporol A or B (Fig. 7**B–D**). It is noteworthy that in this experiment the dosage of cladosporols was lower than the one used in the assay shown in Fig. 6**A** (5 μM versus 10 or 20 μM). In addition, it is remarkable that migration of PC-3 cells, exposed to the conditioned culture medium from cladosporol-treated 3T3-L1 cells and then cultured in medium without cladosporols for additional two days (the samples are denoted as MDI-CL A and MDI-CL B in the scheme of Fig. 7**A and B**), was inhibited in equally strong manner than the cells continuously treated with cladosporols (these samples are denoted as MDI + CL A and MDI + CL B in the scheme

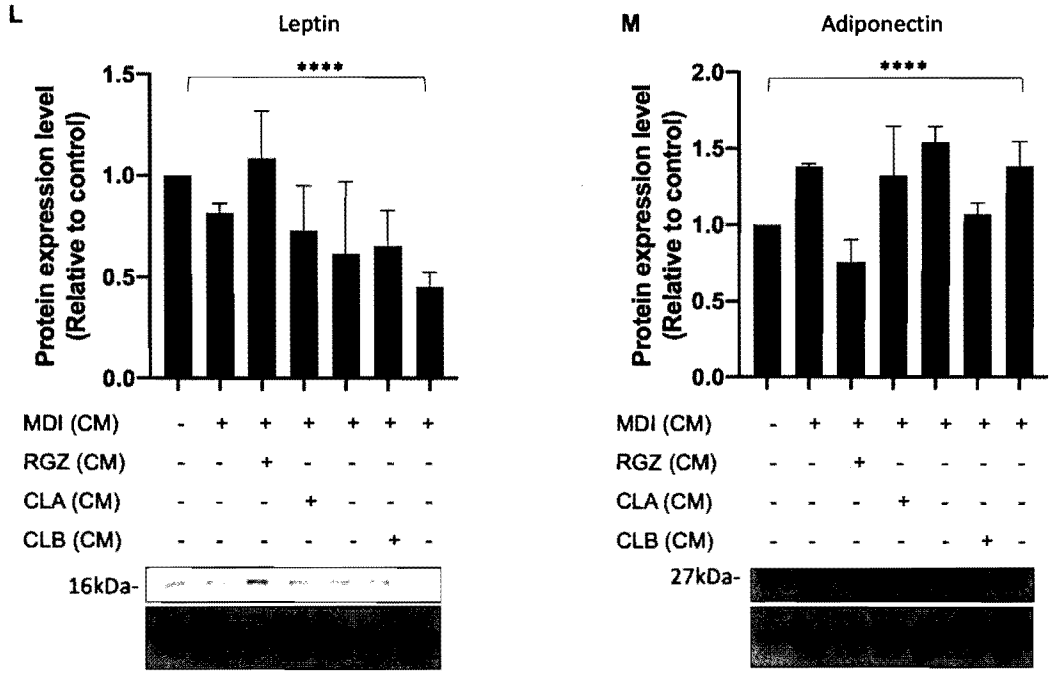

Fig. 8. (*continued*).

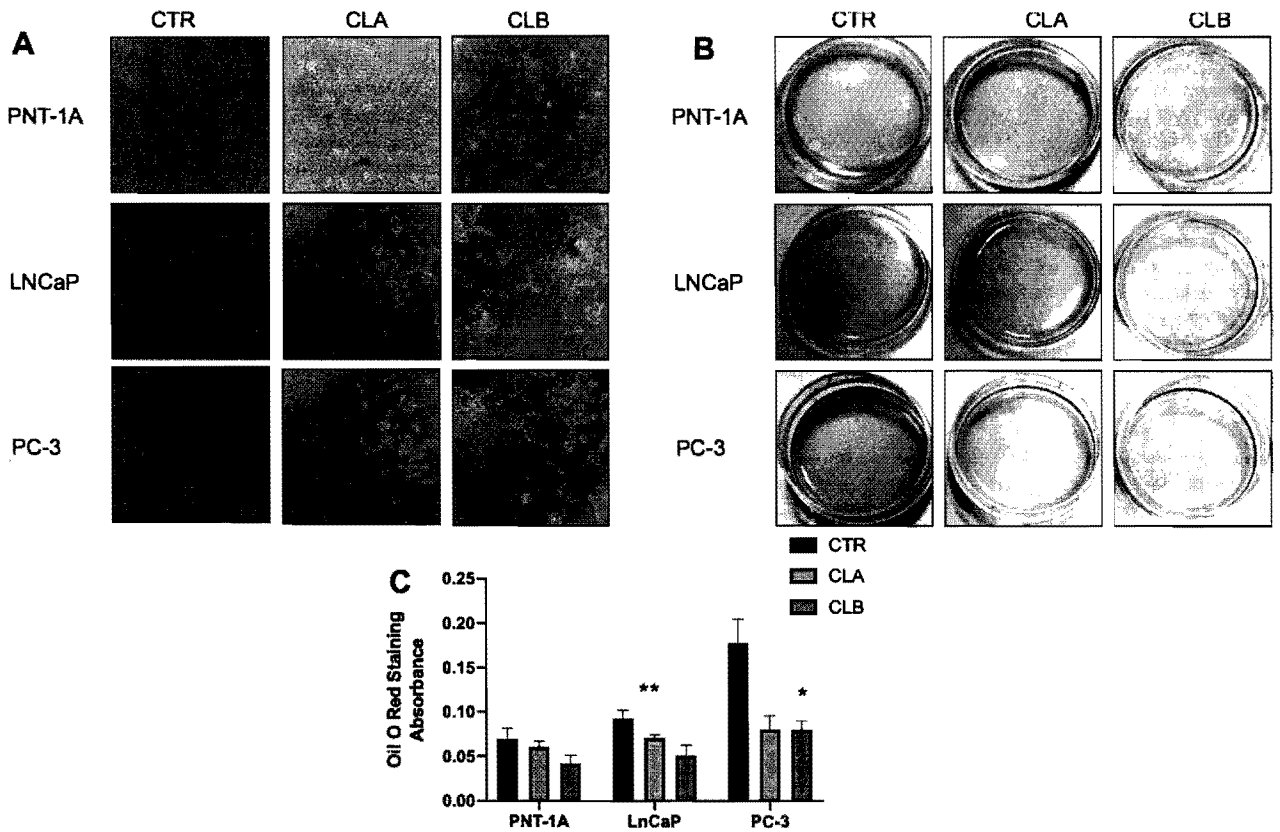

Fig. 9. Cladosporol A and B reduce the accumulation of lipid depots in prostate cancer cells. (A) PNT-1A, LNCaP and PC-3 prostate cells were treated with 10 μM cladosporol A and cladosporol B for 48 hrs and lipid content was stained with Oil Red O. (B) Petri dishes, in which the same cells were treated, were photographed. (C) Quantitative evaluation of the Oil Red O staining elution was reported in the graph. Absorbance was measured at 500 nM. The bar graphs represent the mean ± SD of at least three independent experiments. *$p < 0.05$ **$p < 0.01$ compared to the control.

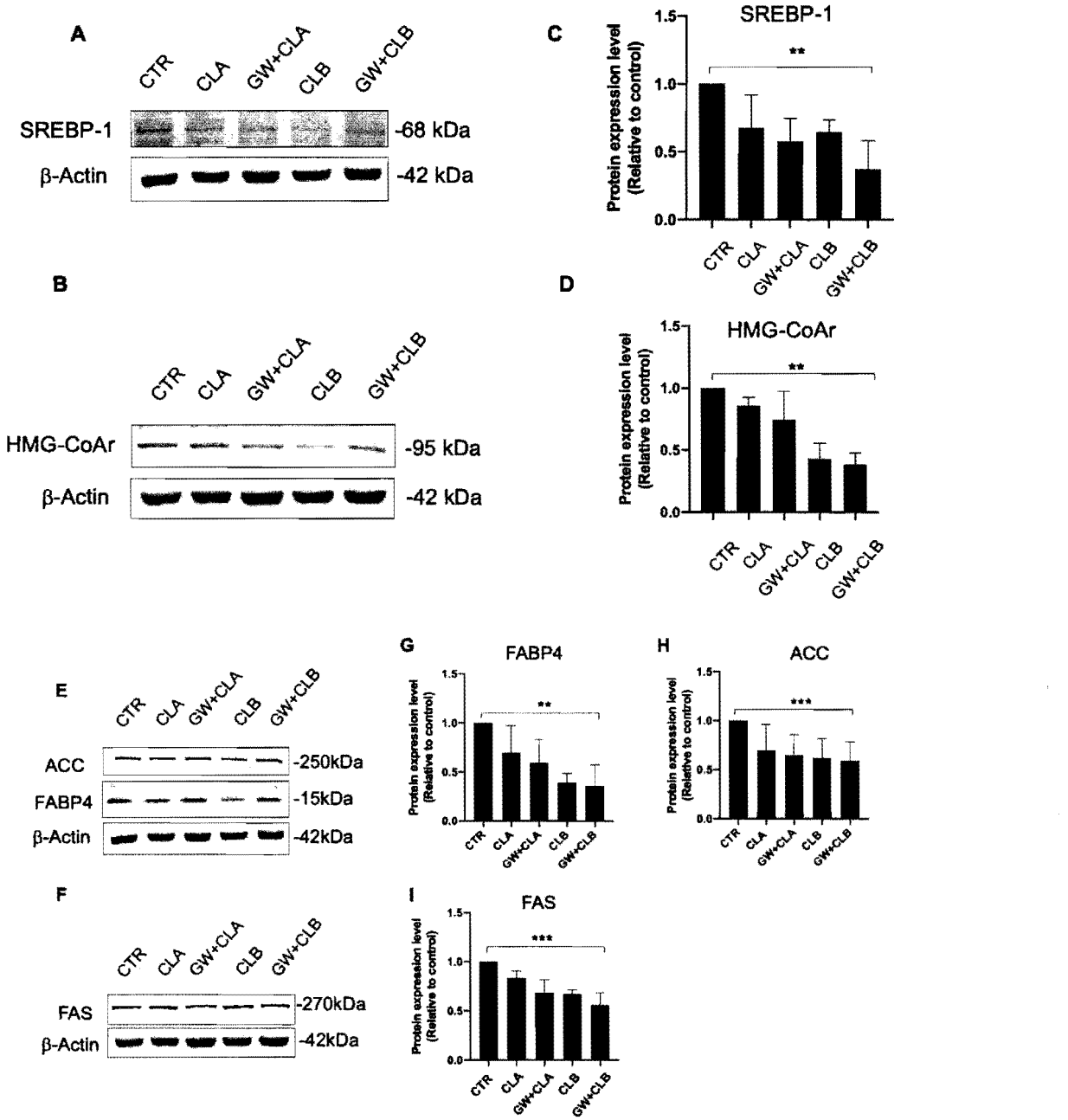

Fig. 10. Cladosporol A and cladosporol B reduced lipid metabolism. (A-D) Western blotting analysis of the expression level of factors involved in the synthesis of cholesterol (SREBP-1; HMG-CoAr) and (E-I) in the synthesis of fatty acids (ACC; FABP4; FAS) on total protein extracts from PC-3 cells pretreated or not with 5 μM GW9662 and then treated with 10 μM cladosporol A and cladosporol B for 48 hrs. Normalization of the loaded samples was performed using an anti-β-actin antibody. The western blotting shown here is only a representative experiment. The bar graphs represent the mean ± SD of protein/β-actin of at least three independent experiments. $^{**}p < 0.01$ $^{***}p < 0.001$ compared to the control.

of Fig. 7**A**). Reduction of β -catenin, cyclin D1, caspase-3 and MMP-9, with the concomitant increase of E-cadherin and cleaved caspase-3 in PC-3 cells, confirmed the involvement of a secreted protein factor as a regulator of prostate cancer cell proliferation. The increase in adiponectin receptor 1 (Adipo-R1) expression in PC-3 cultured in the cladosporol-conditioned medium (Fig. 8**I**) well correlated with the higher amount of adiponectin present in the medium culture derived from 3T3-L1 cells treated with cladosporols (Fig. 8**M**). These results interestingly suggested that adiponectin, synthetized and released in the medium from 3T3-L1 cells treated with cladosporols, broke the dialogue between mature adipocytes and PC-3 cells, in the tumor microenvironment, to inhibit cell proliferation and migration (Fig. 7**B–D**).

Lipid metabolism and cancer are strictly connected and and thereby a dysregulated lipid metabolism is one of the most important hallmark of cancer [50,51]. Tumor cells continously need fatty acids for membrane synthesis to sustain the excessive proliferation rate [52]. Fatty acids biosynthesis requires the transcriptional activation of several genes encoding for specific enzymes involved in this metabolic pathway (ATP cytrate lyase, ACLY; Acetyl-CoA Carboxilase, ACC; Fatty Acid Synthase, FASN). This latter event is mostly dependent on SREBP-1 transcription factor which is also responsible for cholesterol synthesis [53]. In this work, we confirmed that the fundamental prerequisite for prostate carcinogenesis is fat accumulation and that this was counteracted by cladosporol treatments of PC-3 cells (Fig. 9**A–C**). We further demonstrated that fat accumulation correlated with an increase in the expression of enzymes involved in fatty acid and cholesterol

biosynthesis and that cladosporols were able to inhibit not only SREBP-1 itself, but also these specific SREBP-1 targets (FAS, HMG-CoA reductase) (Fig. 10A–I). *De novo* biosynthesis of cholesterol, activated by SREBP-1, has also been shown to support *de novo* intratumoral biosynthesis of androgens occurring during the prostate cancer re-growth, when patients are usually kept in a low concentration condition because they are under hormonal ablation therapy [54,55]. Our data on cladosporol's inhibitory function on PC-3 metastatic prostate cancer-derived cells are very encouraging, because we may hypothesize that, by interrupting the metabolic pathway that induced cholesterol synthesis, we also inhibited the intratumoral *de novo* biosynthesis of androgens. Since PC-3 cells show a reduced concentration of AR, but may display a higher sensitivity to endogeneously produced androgen hormones, the inhibitory action of cladosporols towards these SREBP-1-dependent targets, causing a stronger proliferation arrest of PC-3 cells, can result in even more increased anticancer effect.

Although many studies will be necessary to highlight the different aspects of cladosporol action in the control of initiation and progression of prostate cancer, the results described in this paper are interesting because they stimulate more investigations about these natural molecules that, together with others, could be a part of a new equipment to prevent and treat metastatic prostate cancer. Cladosporols, as therapeutical tools, constitute a good example of new molecules that are recognized as PPARγ ligands and, alone or in combination with conventional anticancer drugs, interfere with two relevant pathological processes, i.e. cell proliferation and lipid pathway dysregulation. Translation of this study in 3D culture and *in vivo* models will be the necessary future step in order to improve the informations about the cladosporol role.

CRediT authorship contribution statement

Roberta Rapuano: Writing – review & editing, Writing – original draft, Methodology, Investigation, Formal analysis. **Alessio Riccio:** Investigation. **Antonella Mercuri:** Investigation. **Jessica Raffaella Madera:** Methodology, Investigation. **Sabrina Dallavalle:** Methodology. **Salvatore Moricca:** Methodology. **Angelo Lupo:** Writing – review & editing, Writing – original draft, Supervision, Methodology, Formal analysis, Conceptualization.

Declaration of competing interest

The authors declare that they have no known competing financial interests or personal relationships that could have appeared to influence the work reported in this paper.

Data availability

The authors do not have permission to share data.

Acknowledgement

We thank Prof. Francesco Beguinot and Prof. Claudia Miele (Department of Translational Medical Sciences, 'Federico II' University of Naples and Istituto per l'endocrinologia e l'Oncologia [IEOS] 'Gaetano Salvatore', Naples, Italy) for technical assistance in setting up the 3 T3-L1 cell differentiation protocol. We also thank Prof. Gabriella Castoria (Università della Campania "L. Vanvitelli" Dip. Medicina di Precisione via L. De Crecchio, 7 80138 Napoli, Italy) for the gift of prostate cancer cells.

This work was supported by funds from DST-University of Sannio (FRA 2020-2021).

References

[1] R.L. Siegel, K.D. Miller, N.S. Wagle, A. Jemal, Cancer statistics, 2023, CA Cancer J. Clin. 73 (2023) 17–48.
[2] ECIS—European Cancer Information System. Prostate Cancer Fact Sheet in 2020. Available online: https://ecis.jrc.ec.europa.eu.
[3] Cheng HH, Nelson PS. Genetic risk factors for prostate cancer. UpToDate. 2019. Accessed at https://www.uptodate.com/contents/genetic-risk-factors-for-prostate-cancer on March 19, 2019.
[4] B. Grundmark, H. Garmo, M. Loda, C. Busch, L. Holmberg, B. Zethelius, The metabolic syndrome and the risk of prostate cancer under competing risks of death from other causes, Cancer Epidemiol. Biomark. Prev. 19 (2010) 2088–2096.
[5] C.S. Langlais, R.E. Graff, E.L. Van Blarigan, N.R. Palmer, S.L. Washington 3rd, J. M. Chan, S.K. Kenfield, Post-diagnostic dietary and lifestyle factors and prostate cancer recurrence, progression and mortality, Curr. Oncol. Rep. 10 (23) (2021) 37.
[6] M. Yang, et al., Dietary patterns after prostate cancer diagnosis in relation to disease-specific and total mortality cancer prev. Philos. Phenomenol. Res. 8 (2015) 545–551.
[7] G. Markozannes, et al., Diet, body size, physical activity and risk of prostate cancer, an umbrella review of the evidence, Euro J. Cancer 69 (2016) 61–69.
[8] M. Chen, et al., An aberrant SREBP-dependent lipogenic program promotes metastatic prostate cancer, Nat. Genet. 50 (2018) 206–218.
[9] J. Chen, I. Guccini, D. Di Mitri, D. Brina, A. Revandkar, M. Sarti, E. Pasquini, et al., Compartmentalized activities of the pyruvate dehydrogenase complex sustain lipogenesis in prostate cancer, Nat. Genet. 50 (2018) 219–228.
[10] S. Noh, E. Choi, C. Hwang, J.H. Jung, S. Kim, B. Kim, Dietary compounds for targeting prostate cancer, Nutrients 11 (2019) 2401–2434.
[11] G.M. Cragg, D.J. Newman, Natural products: a continuing source of novel drug leads, BBA 1830 (2013) 3670–3695.
[12] S. Mondal, S. Bandyopadhyay, M.K. Ghosh, S. Mukhopadhyay, S. Roy, C. Mandal, Natural products: promising resources for cancer drug discovery, Anticancer Agents Med Chem. 12 (2012) 49–75.
[13] E. Ottow, H. Weinmann, Nuclear receptors as drug targets, Wiley-VCH, Germany, 2008.
[14] D. Zurlo, C. Leone, G. Assante, S. Salzano, G. Renzone, A. Scaloni, C. Forestz, V. Colantuoni, A. Lupo, Cladosporol a stimulates G1-phase arrest of the cell cycle by up-regulation of p21waf1/cip1 expression in human colon carcinoma HT-29 cells, Mol. Carcinog. 52 (2013) 1–17.
[15] D. Zurlo, G. Assante, S. Moricca, V. Colantuoni, A. Lupo, A. Cladosporol, a new peroxisome proliferator-activated receptor γ (PPARγ) ligand, inhibits colorectal cancer cells proliferation through β-CATENIN/TCF pathway inactivation, BBA 1840 (2014) 2361–2372.
[16] D. Zurlo, P. Ziccardi, C. Votino, T. Colangelo, C. Cerchia, F. Dal Piaz, S. Dallavalle, S. Moricca, E. Novellino, A. Lavecchia, V. Colantuoni, A. Lupo, The antiproliferative and proapoptotic effects of cladosporols a and B are related to their different binding mode as PPARγ ligands, Biochem. Pharmacol. 108 (2016) 22–35.
[17] R. Rapuano, P. Ziccardi, V. Cioffi, S. Dallavalle, S. Moricca, A. Lupo, Cladosporols a and B, two natural peroxisome proliferator-activated receptor gamma (PPARγ) agonists, inhibit adipogenesis in 3T3-L1 preadipocytes and cause a conditioned-culture-medium-dependent arrest of HT-29 cell proliferation, BBA-General Subjects (2021) 129973.
[18] X. Zhang, G. Zhou, B. Sun, G. Zhao, G. Liu, J. Sun, C. Liu, H. Guo, Impact of obesity upon prostate cancer-associated mortality, a meta analysis of 17 cohort studies, Oncol. Lett. 9 (2015) 1307–1312.
[19] R. Ribeiro, C. Monteiro, V. Cunha, M.J. Oliveira, M. Freitas, A. Fraga, P. Principe, C. Lobato, F. Lobo, A. Morais, V. Silva, J. Sanches-Magalhaes, J. Oliveira, F. Pina, A. Mota-Pinto, C. Lopes, R. Medeiros, Human perirprostatic adipose tissue promotes prostate cancer aggressiveness in vitro, J. Exp. Clin. Cancer Res. 31 (2012) 32.
[20] V. Laurent, A. Guerard, C. Mazerolles, S. LeGonidec, A. Toulet, L. Nieto, F. Zaidi, B. Majed, D. Garandeau, Y. Socrier, M. Golzio, T. Cadoudal, K. Chaoui, C. Bray, B. Mousarrat, O. Schiltz, Y.Y. Wang, B. Couderc, P. Valet, B. Malavaud, C. Muller, Periprostatic adipocytes act as a driving force for prostate cancer progression in obesity, Nat. Commun. 7 (2016) 10230.
[21] P. Tontonoz, B.M. Spiegelman, Fat and beyond: the diverse biology of PPARγ, Annu. Rev. Biochem 77 (2008) 289–312.
[22] B.M.F. Hernandez-Quiles, E. Kalkhoven, PPARgamma in metabolism, immunity, and cancer: unified and diverse mechanisms of action, Front. Endocrinol. 12 (2021) 624112.
[23] J. Gu, M. Xue, Q. Wang, X. Hong, X. Wang, F. Zhou, J. Sun, G. Wng, Y. Peng, Novel strategy of proxalutamide for the treatment of prostate cancer through coordinated blockade of lipogenesis and androgen receptor Axis, Int. J. Mol. Sci. 22 (2021) 13222.
[24] L. Galbraith, H. Leung, Y. Ahmad Imran, Lipid pathway deregulation in advanced prostate cancer, Pharmacol. Res. 131 (2018) 177–184.
[25] M.M. Webber, D. Bello, S. Quader, Immortalized and tumorigenic adult human prostatic epithelial cell lines: characteristics and applications, part 1, cell markers and immortalized nontumorigenic cell lines, Prostate 29 (1996) 386–394.
[26] M.M. Webber, D. Bello, S. Quader, Immortalized and tumorigenic adult human prostatic epithelial cell lines: characteristics and applications, part 2, tumorigenic cell lines, Prostate 30 (1997) 136–142.
[27] G. Nasini, A. Arnone, G. Assante, A. Bava, S. Moricca, A. Ragazzi, Secondary metabolites of Cladosporium tenuissimum, a hyperparasite of rust fungi Phytochemistry 65 (2004) 2104–2111.

[28] S. Monicca, A. Ragazzi, G. Assante, Bioconirol of rust fungi by Cladosporium tenuissimum, in: M. Hao Pei, A.R. McCracken (Eds.), Rust Diseases of Willow and Poplar, CABI Publishing, International, Wallingford, UK, 2005, pp. 213–229.
[29] C.C. Elix, et al., Peroxisome proliferator-activated receptor gamma controls prostate cancer cell growth through AR-dependent and independent mechanisms, Prostate 80 (2020) 162–172.
[30] E. Mueller, et al., Effects of ligand activation of peroxisome proliferator-activated receptor in human prostate cancer, PNAS 97 (2000) 10990–10995.
[31] F. Alimirah, J. Chen, Z. Basrawala, H. Xin, D. Choubey, DU-145 and PC-3 human prostate cancer cell lines express androgen receptor: implications for the androgen receptor functions and regulation, FEBS Lett. 580 (2006) 2294–2300.
[32] E. Olokpa, P.E. Moss, L.V. Steward, Crosstalk between the androgen receptor and PPAR gamma signaling pathways in the prostate, PPAR Res. (2017) 9456020–9456033.
[33] G. Zadra, C. Photopoulos, M. Loda, The fat side of prostate cancer, BBA 1831 (2013) 1518–1532.
[34] M.K. Pandey, S.C. Gupta, A. Nabavizadeh, B.B. Aggarwal, Regulation of cell signaling pathways by dietary agents for cancer prevention and treatment, Semin. Cancer Biol. 46 (2017) 158–181.
[35] M. Danval, Z.A. Siddiqui, M. Akram, H. Asif, S. Sultana, A. Khan, Epidemiology, etiology, diagnosis and treatment of prostate cancer, Asian Pac. J. Cancer Prev. 15 (2014) 9575–9578.
[36] S.W.D. Merriel, G. Funston, W. Hamilton, Prostate cancer in primary care adv, Ther. 35 (2018) 1285–1294.
[37] P.S. Nelson, et al., The program of androgen-responsive genes in neoplastic prostate epithelium, PNAS 99 (2002) 11890–11895.
[38] D.P. Petrylak, Current state of castration-resistant prostate cancer, Am. J. Man. Care. 19 (2013) 358–365.
[39] F. Hong, et al., PPARs as nuclear receptors for nutrient and energy metabolism, Molecules 24 (2019) 2545–2565.
[40] F. Alimirah, et al., DU-145 and PC-3 human prostate cancer cell lines express androgen receptor: implications for the androgen receptor functions and regulation, FEBS Letter 580 (2006) 2294–2300.
[41] K.M. Wadosky, S. Koochekpour, Androgen receptor splice variants and prostate cancer: from bench to bedside', Oncotarget 8 (2017) 18550–18576.
[42] S.M. Delfin, et al., Splicing of a novel androgen receptor exon generates a constitutively active androgen receptor that mediates prostate cancer therapy resistance, Cancer Res. 68 (2008) 5469–5477.
[43] K.E. Ware, et al., Biologic and clinical significance of androgen receptor variants in castration resistant prostate cancer, Endocrine- Related Cancer. 21 (2014) T87–T103.
[44] D.W. Strand, et al., Pparγ Isoforms Differentially Regulate Metabolic Networks to Mediate Mouse Prostatic Epithelial Differentiation Cell Death and Disease 3 (2012) e364.
[45] F. Li, et al., Upregulated PPARG? facilitates interaction with demethylated AKAP12 gene promoter and suppresses proliferation in prostate cancer, Cell Death Dis. 12 (2021) 528.
[46] F. Dong, et al., PPARγ2 functions as a tumor suppressor in a translational mouse model of human prostate cancer, Asian J. Androl. 24 (2022) 90–96.
[47] C. Elix, S.K. Pal, J.O. Jones, The role of peroxisome proliferator activated receptor gamma in prostate cancer, Asian J. Androl. 19 (2017) 1–6.
[48] **Li Z, Takino T, Endo Yand Sato H. Activation of MMP-9 by membrane type-1 MMP/ MMP-2 axis stimulates tumor metastasis. Cancer Sci. 2017; 108: 347–353.**
[49] N. Cui, M. Hu, R.A. Khalil, Biochemical and biological attributes of matrix metalloproteinases, Prog. Mol. Biol. Transl. Sci. 147 (2017) 1–73.
[50] G. Medes, A. Thomas, S. Weinhouse, Metabolism of neoplastic tissue. IV. a study of lipid synthesis in neoplastic tissue slices in vitro, Cancer Res. 13 (1953) 27–29.
[51] D. Hanahan, R.A. Weinberg, Hallmarks of cancer: the next generation, Cell 144 (2011) 646–674.
[52] R.J. De Berardinis, N.S. Chandel, Fundamentals of Cancer Metabolism, Sci. Adv 2 (2016) e1600200.
[53] J.D. Horton, J.L. Goldstein, M.S. Brown, Activators of the complete program of cholesterol and fatty acid synthesis in the liver, J. Clin. Invest. 109 (2002) 1125–1131.
[54] J.L. Mohler, M.A. Titus, S. Bai, B.J. Kennerley, F.B. Lih, K.B. Tomer, Wilson EM activation of the androgen receptor by intratumoral bioconversion of androstanediol to dihydrotestosterone in prostate cancer, Cancer Res. 15 (2011) 1486–1496.
[55] R.B. Montgomery, E.A. Mostaghel, R. Vessella, D.L. Hess, T.F. Kalhorn, C. S. Higano, L.D. True, P.S. Nelson, Maintenance of Intratumoral Androgens in Metastatic Prostate Cancer: a Mechanism for Castration-Resistant Tumor Growth Cancer Res. 68 (2008) 4447–4454.